

The Journal of Island and Coastal Archaeology

ISSN: (Print) (Online) Journal homepage: www.tandfonline.com/journals/uica20

From earth to sky: Large-scale archaeological settlement patterns in southernmost South America based on ground surveys, UAV LiDAR, and open access satellite imagery

Jo Sindre P. Eidshaug, Hein B. Bjerck, Heidi M. Breivik, Ole Risbøl, Angélica M. Tivoli & Atilio Francisco J. Zangrando

To cite this article: Jo Sindre P. Eidshaug, Hein B. Bjerck, Heidi M. Breivik, Ole Risbøl, Angélica M. Tivoli & Atilio Francisco J. Zangrando (09 Dec 2024): From earth to sky: Large-scale archaeological settlement patterns in southernmost South America based on ground surveys, UAV LiDAR, and open access satellite imagery, The Journal of Island and Coastal Archaeology, DOI: 10.1080/15564894.2024.2426828

To link to this article: https://doi.org/10.1080/15564894.2024.2426828

© 2024 The Author(s). Published by Informa UK Limited, trading as Taylor & Francis Group

Published online: 09 Dec 2024.

Submit your article to this journal

Article views: 66

View related articles

View Crossmark data

Full Terms & Conditions of access and use can be found at
https://www.tandfonline.com/action/journalInformation?journalCode=uica20

THE JOURNAL OF ISLAND AND COASTAL ARCHAEOLOGY
https://doi.org/10.1080/15564894.2024.2426828

Routledge
Taylor & Francis Group

OPEN ACCESS Check for updates

From earth to sky: Large-scale archaeological settlement patterns in southernmost South America based on ground surveys, UAV LiDAR, and open access satellite imagery

Jo Sindre P. Eidshaug[a], Hein B. Bjerck[a], Heidi M. Breivik[a], Ole Risbøl[a], Angélica M. Tivoli[b], and Atilio Francisco J. Zangrando[b]

[a]Department of Archaeology and Cultural History, NTNU University Museum, Norwegian University of Science and Technology (NTNU), Trondheim, Norway; [b]Centro Austral de Investigaciones Científicas, Consejo Nacional de Investigaciones Científicas y Técnicas (CADIC-CONICET), Ushuaia, Tierra del Fuego, Argentina

ABSTRACT

Large-scale archaeological surveys in coastal areas can be challenging. Factors such as remoteness, logistics, accessibility, and weather conditions can render fieldwork time-consuming and expensive in rugged archipelagic settings. Remote sensing encompasses several methods that can be used for increasing the survey area and promoting new archaeological insights. Moreover, it can be an affordable option. Google Earth (among others) collects aerial and satellite imagery from third parties and makes them freely available from anywhere in the world. In southern Tierra del Fuego, clusters of ring-shaped shell middens are conspicuous archaeological features. They are abundant in the central part of the Beagle Channel, but it has not been feasible to study their distribution across the Fuegian archipelago because we lack data from many remote areas where fieldwork is not easily conducted. Remote sensing provides a viable option for large-scale surveying due to the general visibility of these midden clusters. In this study, we establish confidence in open access satellite imagery identifications of ring-shaped middens in Tierra del Fuego based on comparisons with UAV LiDAR and conventional ground surveys, arguing that the results are appropriate for studies of large-scale trends. We provide the results from a full desk-based survey of satellite imagery provided by Google Earth, ESRI, and Microsoft Bing, covering 3000 km of coastline up to 1 km inland in southern Tierra del Fuego. Moreover, we determine the geographical distribution of ring-shaped middens and explore large-scale trends in coastal settlement patterns and landscape use—showing that ring-shaped middens are not evenly distributed across the Fuegian archipelago but strongly related to the sheltered areas of the Beagle and Murray Channels.

ARTICLE HISTORY
Received 21 December 2023;
Accepted 10 August 2024

KEYWORDS

Google Earth; coastal archaeology; landscape use; shell middens; Tierra del Fuego

Introduction

Worldwide, shell middens are a foundational component of coastal archaeological research (Rick 2024; Waselkov 1987). In South America, these cultural accumulations

CONTACT Jo Sindre P. Eidshaug jo.eidshaug@ntnu.no; josindree@outlook.com Department of Archaeology and Cultural History, NTNU University Museum, Norwegian University of Science and Technology (NTNU), 7491 Trondheim, Norway

© 2024 The Author(s). Published by Informa UK Limited, trading as Taylor & Francis Group
This is an Open Access article distributed under the terms of the Creative Commons Attribution License (http://creativecommons.org/licenses/by/4.0/), which permits unrestricted use, distribution, and reproduction in any medium, provided the original work is properly cited. The terms on which this article has been published allow the posting of the Accepted Manuscript in a repository by the author(s) or with their consent.

can range in size from a few centimeters to approximately 30 m in height, have diverse shapes, and contain varied proportions of sediments, shells, cultural materials, and features (Zangrando 2018). In southern Tierra del Fuego (Argentina and Chile), shell middens are by far the most common archaeological features and they are particularly abundant in the more sheltered, central part of the Beagle Channel (Orquera, Legoupil, and Piana 2011; Zangrando 2018). Here, the Norwegian–Argentinean research collaboration Marine Ventures (Bjerck, Breivik, et al. 2016; Bjerck and Zangrando 2013) recorded more than 1200 middens within 3 km^2 surrounding Cambaceres Bay during thorough field surveys in 2009–2013 (i.e., the Cambaceres surveys; Figure 1) (Bjerck, Zangrando, et al. 2016). However, archaeological surveys along coasts and on islands in regions such as Tierra del Fuego can be demanding—especially at scales that are relevant for examining large-scale coastal settlement patterns. Complexity and density of archaeological remains, remoteness, logistics, accessibility, and weather conditions are factors that can contribute to render fieldwork a time-consuming and expensive enterprise. Thus, with a few exceptions (e.g., see Barceló, Piana, and Martinioni 2002; Bjerck, Zangrando, et al. 2016; Ocampo and Rivas 2004; Risbøl et al. 2023), large-scale settlement patterns and distribution of shell middens have rarely been studied in southern Tierra del Fuego. And there is a sense of urgency in recording and monitoring cultural heritage in coastal and island environments globally, as it is vulnerable to the effects of global warming, such as rising sea levels and coastal erosion (Erlandson 2008, 2012).



Figure 1. Map of Tierra del Fuego with some of the places mentioned in the text. The Beagle Channel can be separated in the western, central, and eastern part. Source: Esri, Maxar, Earthstar Geographics, and the GIS User Community. Illustration: Jo Sindre P. Eidshaug.

In this study, we use remote sensing as a means to tackle challenges related to fieldwork in coastal settings and as a novel approach to map and study the geographical distribution of shell middens in southern Tierra del Fuego at a macro-regional scale. Archaeological remote sensing is materializing as a field of research that promotes novel ways of addressing and understanding the past (e.g., Casana 2021; Chase et al. 2012; Comer and Harrower 2012; Luo, Wang, Guo, et al. 2019; Opitz and Cowley 2013; Vinci et al. 2024). One key advantage of this technology is scale. Air- and spaceborne remote sensing enables large-scale, nondestructive identification of archaeological features, even in remote places, and allows addressing certain archaeological issues pertaining to geospatial scales that are nearly unthinkable in conventional fieldwork (e.g., see Howey et al. 2020; Menze and Ur 2012; Stoner 2017; Stott, Kristiansen, and Sindbæk 2019). Additionally, remote sensing need not be expensive. In many areas, resolution of open data has improved to a level that allows moving beyond mere detection to relatively detailed large-scale landscape studies (Borie et al. 2019; Davis and Douglass 2020; Hritz 2014). Moreover, some software platforms are intuitive and easy-to-use. Virtual globes, such as Google Earth, ESRI World Imagery Wayback, and Microsoft Bing Maps collect aerial and satellite data from various sources to make free, multi-resolution satellite imagery with almost unlimited coverage publicly available (Luo et al. 2018). And due to the general visibility of shell middens in Tierra del Fuego, remote sensing provides a viable option for large-scale surveying in this area.

While the Beagle Channel region is dominated by mixed deciduous and evergreen Nothofagus forests, archaeological sites are often located in open coastal areas with scattered shrubs and trees—providing favorable conditions for remote sensing. In 2022, Marine Ventures carried out an unmanned aerial vehicle (UAV) light detection and ranging (LiDAR) survey on the Argentinean coast of the Beagle Channel (Risbøl et al. 2023). The $\sim$12 km^2 surveyed area included that covered by the Cambaceres surveys. A comparison with the ground survey record from Cambaceres Bay showed that 69% of the shell middens were identified on UAV LiDAR. For the most numerous category, *ring-shaped shell middens* (i.e., middens arranged around dwelling huts), the detection rate was as high as 83%.

This paper takes comparison one step further by including satellite imagery available through Google Earth, ESRI, and Microsoft Bing.[1] Satellite imagery allows us to expand the study area dramatically—to a macro-regional scale. Although Google Earth only provides red, green, and blue (RGB) composite images and no multi-spectral information (Luo et al. 2018), studies in other parts of the world have shown that it can be a useful tool for large-scale archaeological prospection of structures that have high visibility and are not covered by vegetation (e.g., Kennedy and Bishop 2011; Luo, Wang, Liu, et al. 2019; Sadr 2016)—though some kind of field validation is required (Luo et al. 2018).

The main purpose of this paper is to explore the geographical distribution of ring-shaped middens and large-scale trends in coastal settlement patterns and landscape use in southern Tierra del Fuego based on ground surveys, UAV LiDAR, and open access satellite imagery. To do so, we assess the information loss for each step up from the ground—i.e., ground (field survey), air (UAV LiDAR survey), and thermosphere/low Earth orbit (satellite imagery survey)—and argue that open access satellite imagery

(Google Earth, supplemented by ESRI and Microsoft Bing) provides appropriate information for large-scale, macro-regional analyses of coastal settlement patterns and structure along 3000 km of coastline in southern Tierra del Fuego. Using the information from the survey of open access satellite imagery, we show that shell middens are far from evenly distributed across southern Tierra del Fuego and that the abundant and important category of ring-shaped shell middens is clearly related to sheltered areas in the Beagle and Murray Channels and especially concentrated on, and in proximity to, Gable Island in the Beagle Channel (Figure 1). Interestingly, the distribution of ring-shaped middens also differs from the historical territories of the Indigenous groups reported in literature from the nineteenth and early twentieth centuries (see Hyades and Deniker 1891; Lothrop 1928).

The objectives of this study are to: (1) estimate confidence in open access satellite imagery identifications of ring-shaped middens in Tierra del Fuego based on comparisons with ground survey ($\sim$3 km^2) and UAV LiDAR survey ($\sim$12 km^2) records; the study is focused on ring-shaped middens because they make up the most numerous, characteristic, and visible category of shell middens in Tierra del Fuego; (2) determine the geographical distribution of the ring-shaped midden tradition based on results from the survey of open access satellite imagery (3000 km of coastline); and (3) explore large-scale trends in settlement patterns/structure and landscape use in southern Tierra del Fuego based on locations and distribution of the ring-shaped middens identified in satellite imagery.

Research background

LiDAR, open access satellite imagery, and Big Data

The advantages and drawbacks of satellite imagery do not necessarily coincide with other remote sensing techniques, including LiDAR (Sadr 2016; Thuestad et al. 2021). LiDAR is an active remote sensing method for acquiring accurate, high-resolution measurements of the earth's surface based on backscattered laser pulses deployed from a sensor mounted on a terrestrial, airborne, or spaceborne vehicle. Its applicability for archaeological prospection is enhanced by the laser's ability to penetrate high vegetation, which enables ground surface 3D modeling devoid of vegetation (Casana et al. 2021; Doneus and Briese 2011; Risbøl 2013). LiDAR has proven highly useful for archaeology in many contexts across the globe (e.g., Chase et al. 2012; Evans et al. 2013; Iriarte et al. 2020; Opitz and Cowley 2013; for a recent global review, see Vinci et al. 2024) and, albeit still limited in number, applications of LiDAR in shell midden research have increased over the last few years. In addition to a recent study from Tierra del Fuego (Risbøl et al. 2023), this includes investigations of spatial distributions of shell rings in coastal South Carolina using automated LiDAR analyses and deep learning (Davis et al. 2021; Davis, Lipo, and Sanger 2019; Davis, Sanger, and Lipo 2019), and mapping of shell mounds on the Cape York Peninsula, Australia (Emmitt et al. 2020), freshwater shell mounds in northeastern Florida (Randall 2014), and complex shell-midden architecture on the Florida Gulf Coast, using UAV LiDAR (Barbour et al. 2019).

Unlike active remote sensing methods, which measure backscatter reflected from pulses emitted from the sensors' own light sources, passive remote sensing methods only

measure reflected sunlight. Thus, as a passive method based on optical sensors, satellite imaging cannot provide access to surfaces covered by high vegetation. Nevertheless, even open, easy-to-use satellite imagery accessed through Google Earth (and other data repositories) has proved useful for identifying archaeological features with high visibility (e.g., Bewley et al. 2016; Kempe and Al-Malabeh 2013; Luo et al. 2018; Luo, Wang, Liu, et al. 2019; O'Reilly and Scott 2015; Ranzi, Feres, and Brown 2007; Snyder and Haas 2024) and for monitoring landscape and cultural heritage using multi-temporal images (e.g., Contreas 2010; Khalaf and Insoll 2019; Luo et al. 2018; Parcak et al. 2016). Most importantly, however, satellite imagery enables large-scale, rapid, cost-effective desktop surveying—even in remote, inaccessible, and little-explored areas (e.g., Bewley et al. 2016; Kennedy and Bishop 2011; Khalaf and Insoll 2019).

LiDAR coverage is increasing globally but data are still lacking in many places (Cohen, Klassen, and Evans 2020, Figure 1; Risbøl et al. 2023; Vinci et al. 2024), and commissioning LiDAR data may not be viable due to the high associated cost. Collecting commercial satellite data can also be expensive and time-consuming. As such, Google Earth (https://earth.google.com), ESRI (https://livingatlas.arcgis.com/wayback), and Microsoft Bing (https://www.bing.com/maps) (among others) are important alternatives that provide to the public free satellite and aerial imagery and software with intuitive tools (Luo et al. 2018; for a list of open access data repositories and software platforms, see Davis and Douglass 2020, Table 1; Lindsay and Mkrtchyan 2023, Table 1; for overviews of public geospatial data hosted on the freely available cloud-based platform Google Earth Engine, see Gorelick et al. 2017, Table 1; Herndon et al. 2023, Table 1).

One drawback with open access satellite and aerial image subsets is the significant but rather arbitrarily distributed variations in spatial and temporal resolutions of the available imagery from different areas across the globe (Casana 2021; Luo et al. 2018). For instance, the mosaics from southern Tierra del Fuego only consist of satellite images with various spatial and temporal resolutions and no high-resolution aerial imagery (as is more common in urbanized areas). Consequently, it is relevant to conceive satellite

Table 1. Survey areas and datasets included in the study.

Name	Dataset ID	Dataset confidence	Description	Area	Coverage
Ground survey	CG	1	Cambaceres Bay	~3 km^2	CG, LiDAR, GEM
UAV LiDAR survey	LiDAR	2	Brown Bay, Cambaceres Bay, Gable Island NE, Gable Island SE, Moat Bay	~12 km^2	LiDAR, GEM
Google Earth desktop survey, supplemented by ESRI and Microsoft Bing imagery	GEM	3	The coastline of southern Tierra del Fuego, between the southern coast of Isla Grande de Tierra del Fuego (Point Divide–Aguirre Bay) and most of the Cape Horn archipelago, excluding Ushuaia and Puerto Williams	~3000 km (200–1000 m wide corridor)	GEM

Relative confidence in the datasets is ranged from 1 to 3, where 1 is highest.

imagery (particularly from free services) as Big Data (i.e., data that not only are big but inherently patchy, messy, and uncertain) (Bevan 2015).

Big Data is usually perceived in terms of the immense volume, highly fluctuating nature of the data (kind, source, and quality), and high-velocity data capture—offering new forms of opportunities and challenges, and requiring novel approaches (Gattiglia 2015). Remotely Sensed Big Data (RSBD) refers to large-scale geospatial data collected with satellite or airborne sensors, comprising increased spatial extent and resolution, as well as multi-temporal and multi-spectral coverage (Herndon et al. 2023; Howey et al. 2020). Google Earth imagery is generally of a resolution that allows for relatively detailed landscape studies but varies greatly across the globe. Images captured at different times appear next to one another, creating a patchwork of spatial resolutions that can vary from 0.15 to 15 m (Luo et al. 2018). Even though multi-temporal imagery usually is available (e.g., through Google Earth's history-function or ESRI's World Imagery Wayback), serendipity still plays an important role since comparable resolution and quality across larger regions is only rarely available. Moreover, identification of archaeological structures from satellite or aerial imagery is always influenced by uncontrollable factors, such as surface visibility, vegetation, weather (clouds, shadows, snow), etc.—and these vary from image to image while metadata for the original imagery is often lacking (Luo et al. 2018). However inevitable, handling highly mixed information is the price for exploiting the potentials of Big Data (Gattiglia 2015), and a loss of accuracy at the micro-level can often be remedied by insights at the macro-level (Mayer-Schönberger and Cukier 2013, 13–4).

Nevertheless, the label "Big Data" does not issue a free pass to eschew data reliability controls. Jeremy Huggett (2020) argues that the incomplete and often unreliable nature of Big Data makes it no different from archaeological data in general. Failure to recognize this parallel has led to false expectations about Big Data acting as a prime mover in a shift from theory-/hypothesis-driven research toward data-driven research that somehow "magically" can bypass traditional scientific procedures of data quality control (Huggett 2020). Although large, messy sets with lower data quality can yield results as interesting and important as small sets with high-quality data (Gattiglia 2015), it would be illusory to believe that quantity somehow eludes problems pertaining to data quality (Huggett 2020, 59).

For that reason, we evaluate the quality of open access satellite data from southern Tierra del Fuego based on thorough comparisons with ground survey records of $\sim$3 km^2 (Bjerck, Zangrando, et al. 2016) and UAV LiDAR survey records of $\sim$12 km^2 (Risbøl et al. 2023). And while comparing and contrasting these three datasets forms an integral component of data confidence assessment, our case study from Tierra del Fuego aims to show that such use of small datasets with higher confidence can ensure methodically sound applications of "messy" Google Earth data.

Archaeological and ethnographic research

Situated at the southern tip of South America (Argentina and Chile), Tierra del Fuego is exposed both to the Atlantic and Pacific oceans. Notorious for its gales, storms, and troublesome waters, the many islands, fjords, channels, bays, and coves in Tierra del

Fuego offer the outermost protected waters and safe harbors. Most archaeological sites are located in the sheltered, central part of the Beagle Channel (Orquera and Piana 2015, 32–3), which carves through the Andean Mountain Range and separates Isla Grande de Tierra del Fuego from Navarino Island and the Cape Horn archipelago (Figure 1).

Tierra del Fuego hosts a diverse marine ecosystem, which includes whales, seals, fish, seabirds, and shellfish. The importance of the marine resources is materialized in the countless shell middens that punctuate the coasts—testifying to viable and stable relations between humans and marine environments that lasted for millennia (Eidshaug et al. 2024; Orquera and Piana 2009). The archaeological record of southern Tierra del Fuego is primarily confined to coastal areas. Most shell middens are located below 10 m above sea level (a.s.l.) and more than 80% appear within 100 m from the coastline in the Beagle Channel region (Barceló, Piana, and Martinioni 2002; Orquera and Piana 2009).

In the Fuegian archipelago, different kinds of shell midden structures are recorded from ca. 7200 cal BP until recent historical times—the oldest ones being approximately contemporaneous with the Holocene marine transgression maximum (Orquera and Piana 2020; Zangrando et al. 2022; see Björck et al. 2021). In 2002, 641 archaeological sites (mainly clusters of ring-shaped middens) were reported on Navarino Island, Chile, of which 419 were located on the northern coast (Beagle Channel), 110 on the western coast (Murray Channel), and 112 on the southern coast (Ocampo and Rivas 2002, 98–9). By 2010, the number of recorded shell midden sites had reached "nearly a thousand" on the Argentinean coast of the Beagle Channel (Piana and Orquera 2010, 263). Shell middens are also found in the far east, on Peninsula Mitre (Vázquez et al. 2007; Zangrando, Vázquez, and Tessone 2011), and multiple sites have been recorded farther south, on the Cape Horn archipelago (Legoupil 1993–1994; Orquera, Legoupil, and Piana 2011)—even close to Cape Horn (Buma et al. 2022). Shell middens are also common archaeological features north of the Beagle Channel, in the Western Channels, like the Magellan Strait and the Otway and Skyring sounds (Legoupil 2000; San Román et al. 2016).

The Indigenous people of the southernmost South America are the Yagan—also referred to as Yahgan, Yaghan, Yamana, and "canoe people" in ethnographic and scientific literature. In the post-contact era (sixteenth–twentieth centuries), the Yagan still engaged in traditional nomadic marine lifestyles, inhabiting the coastal areas between the southern coast of Isla Grande and Cape Horn (Figure 2). The eastern and western limits of their territory are disputed and partly contradictory in ethnographic sources (Orquera and Piana 2015, 78–84). Peninsula Mitre, at the eastern end of Tierra del Fuego, is generally associated with the Haush—pedestrian hunter-gatherer and fishers with a strong emphasis on exploitation of coastal resources (Bridges 2007; Chapman and Hester 1973; Vidal 2011). However, an ethnographic map by Hyades and Deniker (1891, 425, see also 15, 405) indicated that the Yagan territory extended to Valentin Bay on Peninsula Mitre. According to various sources, the southern coast of Isla Grande between Harberton (Brown Bay) and Sloggett Bay (or Aguirre Bay) was used by both the Yagan and the Selk'nam (terrestrial hunter-gatherers inhabiting the steppes farther north on Isla Grande) in historical times (Gusinde 1937, 234–5; Lothrop 1928; Orquera and Piana 2015, 78–80).

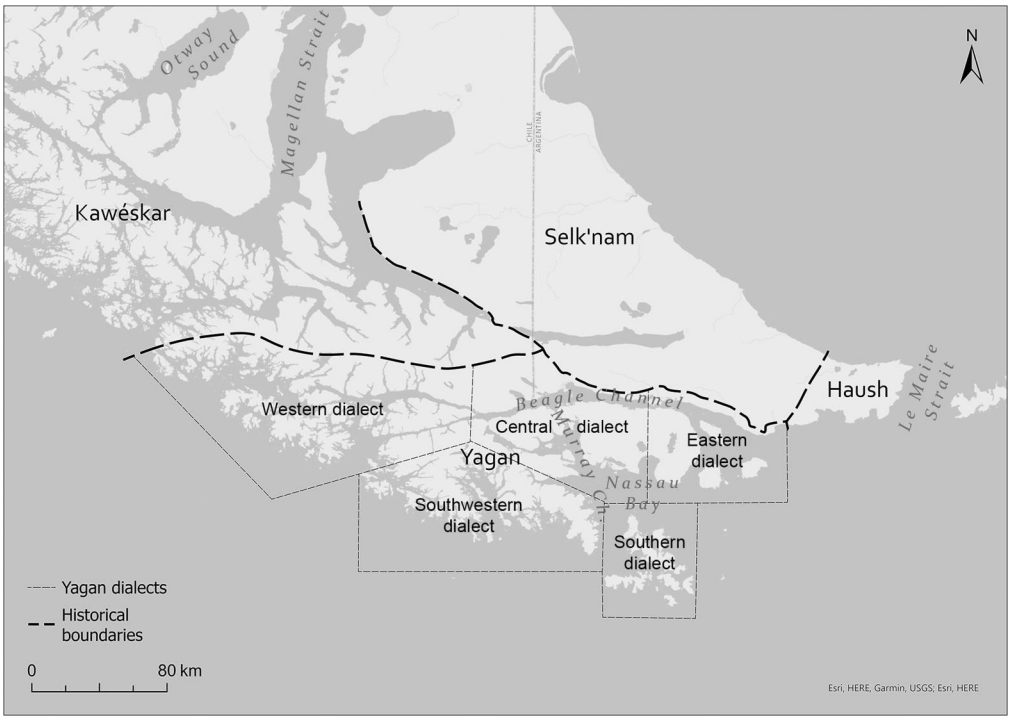


Figure 2. Historical boundaries between ethnic groups and Yagan dialects, based on Lothrop (1928, 24). The most populous of these districts in the post-contact era was undoubtedly the Beagle and Murray channels (Orquera and Piana 2015, 86–90). Source: Esri, HERE, Garmin, OpenStreetMap contributors, and GIS user community. Illustration: Jo Sindre Eidshaug.

In the west, Peninsula Brecknock is traditionally recognized as the border between Yagan and Kawéskar territories—though ethnographic sources indicate that the Kawéskar also used the territory south of Peninsula Brecknock (Borrero, Morello, and San Román 2020, 49; Martinic 1989; Orquera and Piana 2015, 80–3). Territorial differences also existed within the Yagan area and are partly reflected in the presence of five linguistic dialects in historical times (Figure 2) (Gusinde 1937, 199–208; Koppers 1927; Lothrop 1928, 120; Orquera and Piana 2015, 512–8).

Two main factors emerge from this background information. First, during the short period documented by the ethnographic information, a variable panorama is observed in the territorial delimitation of the native groups of southern Tierra del Fuego. Although it is feasible that cultural changes, including territorial reorganization, accelerated during the contact period, a significant variability during the thousands of years represented in the archaeological sequence of the region is also expected (Borrero and Martin 2023). Second, according to archaeological and ethnographic information, all hunter-gatherer-fisher groups in southern Tierra del Fuego included the formation of shell middens.

Ring-shaped shell middens

Shell middens vary in shape and size across the Fuegian archipelago, but one category is particularly conspicuous: ring-shaped shell middens (i.e., shell middens arranged



Figure 3. A small cluster of ring-shaped middens on the northern coast of the Beagle Channel, near Ushuaia, presumably originating from several short-term occupations. The cultural practice of arranging middens around the dwelling huts left visible depressions in the middle of the midden formations. Photo: Jo Sindre P. Eidshaug.

around visible dwelling structures; Figure 3) (Piana and Orquera 2010). Ring-shaped middens are more abundant than other midden types in this region and they mostly appear in clusters close to the shore (Barceló, Piana, and Martinioni 2002; Bjerck, Zangrando, et al. 2016; Ocampo and Rivas 2004; Risbøl et al. 2023). Clusters may count more than 100 interconnected shell rings (i.e., circular depressions enclosed or semi-enclosed by middens; Figure 4).

Ring-shaped middens result from a cultural practice of depositing waste around the dwellings that accumulated to form ring-shaped, sheltering walls (Piana and Orquera 2010; Zangrando 2018). According to ethnographic sources, dwelling huts (constructions of saplings covered by branches, grass, and skins, usually with a base diameter of 3–4 m) were placed within the depressions in the middle of the shell middens (Figure 5). Repeated reuse of the foundations for new huts sustained the midden walls, which kept increasing throughout time. This tradition of reuse made clusters of ring-shaped middens swell out as new dwellings were added adjacent to older midden walls (Piana and Orquera 2010). Based on morphology, ring-shaped middens have typically been distinguished from dome-shaped middens (i.e., shell mounds of various sizes that have no visible traces of dwellings). While the presence or absence of a dwelling adjacent to the midden also is important for the distinction between the two (see Risbøl et al. 2023), it should be noted that dwelling spaces have also been recorded adjacent to dome sites (Zangrando et al. 2014).



Figure 4. Two very large clusters of ring-shaped middens located close to the shoreline in open bays: (A) Wikirrh, Cambaceres Bay. Photo: Jo Sindre P. Eidshaug; (B) a very large site on the southeastern coast of Gable Island. Photo: Magnar M. Gran.

Despite the substantial size of many clusters of ring-shaped middens, ethnographic and archaeological data do not indicate that these settlements were occupied simultaneously by more than a few families except on special occasions, such as when a stranded whale attracted large crowds (Orquera and Piana 1999, 268; Piana and Orquera 2010).

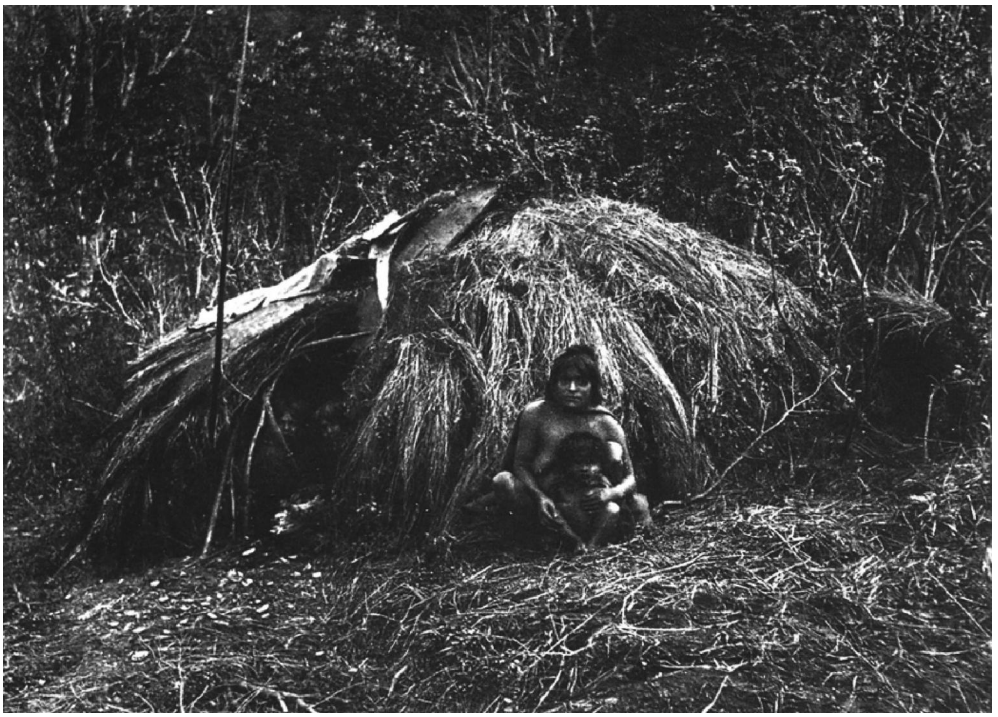


Figure 5. Yagan late nineteenth century traditional dwelling hut with shells deposited in front of the entrance. Photo: Jean Louis Doze and Edmond Payen, 1882–1883.

Archaeological and ethnographic sources show that the Fuegians were mobile marine foragers—their major food sources were marine mammals, guanacos, fish, birds, and shellfish, and their settlements were temporary, only to accumulate over time through intensive reuse of the same locations over short periods, even after long hiatuses (Zangrando 2018). Their reliance on seaborne mobility in subsistence strategies suggests that boats had a decisive impact on settlement structure (Bjerck 2017).

The Cambaceres surveys (2009–2013)

The present study begins with the Cambaceres surveys (2009–2013) recording 1237 shell middens within a 3 km^2 area surrounding Cambaceres and Imiwaia bays (Figure 6) (Bjerck, Zangrando, et al. 2016). The area has a long occupational history which lasted until recent times. The oldest shell midden context, dated to ca. 7250 cal BP (Imiwaia I),[2] is about contemporary with the maximum marine transgression, when the local shorelines were 5 m higher than today (Zangrando et al. 2016).

The Cambaceres surveys report indicated a relation between shell midden category and location (Bjerck, Zangrando, et al. 2016, 75–6): ring-shaped middens[3] ($n = 804$) are structured in aggregations and most abundant near the beach while dome-shaped middens ($n = 432$) are more widely distributed and more often located on coastal drumlin ridges. Note that domes also appear near ring-shaped structures and that a few ring-shaped middens were recorded on ridges.

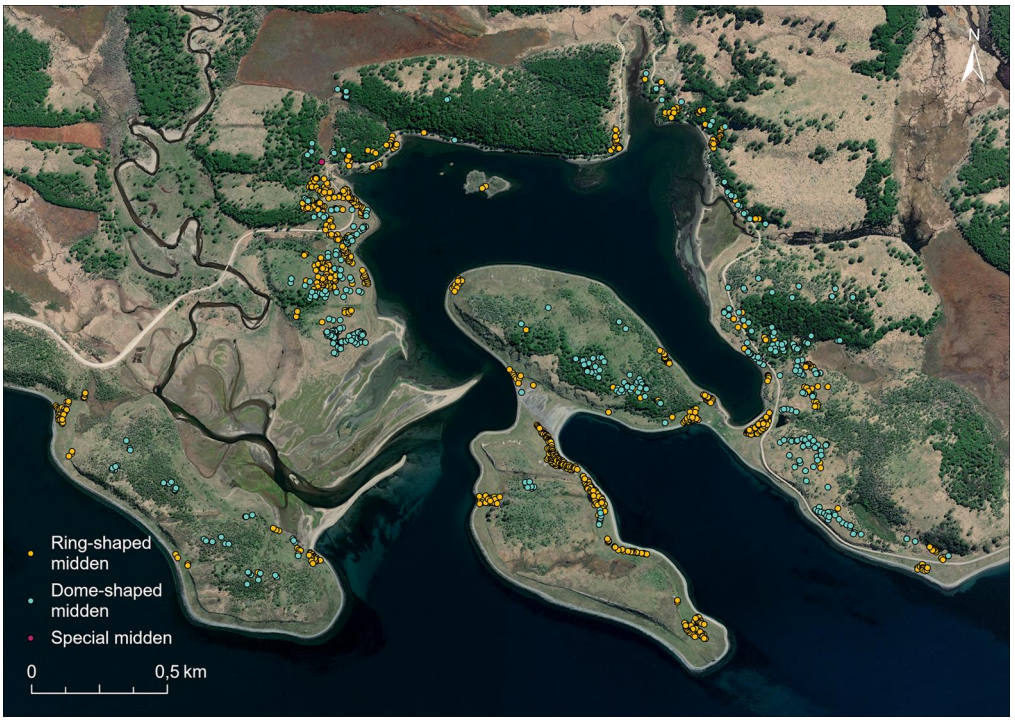


Figure 6. Shell middens recorded in the Cambaceres surveys (2009–2013). Based on Bjerck, Zangrando, et al. (2016). Source: Esri, Maxar, Earthstar Geographics, and the GIS User Community. Illustration: Jo Sindre P. Eidshaug.

The report additionally delivered a brief preliminary analysis of Google Earth imagery from the central part of the Beagle Channel—shedding light on the potentials of applying satellite data in large-scale regional analysis of settlement structure, logistics, and subsistence patterns (Bjerck, Zangrando, et al. 2016, 76–9). Cambaceres Bay hosted one of the largest concentrations of ring-shaped middens and the preliminary analysis indicated a positive relation between good natural harbors and large clusters. Due to the absence of such clusters in the more exposed areas of the Beagle Channel farther east, it was suggested that sheltered sea and reliable harbors were among the defining criteria for the ring-shaped midden tradition, confining it to the Beagle Channel region (Bjerck, Zangrando, et al. 2016, 77). The present study intends to elaborate on these preliminary results by including a more thorough analysis of open access satellite imagery.

Methods

The datasets from the respective areas covered by the Cambaceres and UAV LiDAR surveys were used in the comparison with the desktop survey of satellite imagery from Google Earth, ESRI, and Microsoft Bing (Table 1, Figure 7). The study area for the survey of satellite data was selected based on current knowledge of the distribution of shell middens in southern Tierra del Fuego, as described above. We included a wide area surrounding the Beagle Channel—the area with the most comprehensive record—which covered large parts of Peninsula Mitre and the Cape Horn archipelago (Figure 8). The

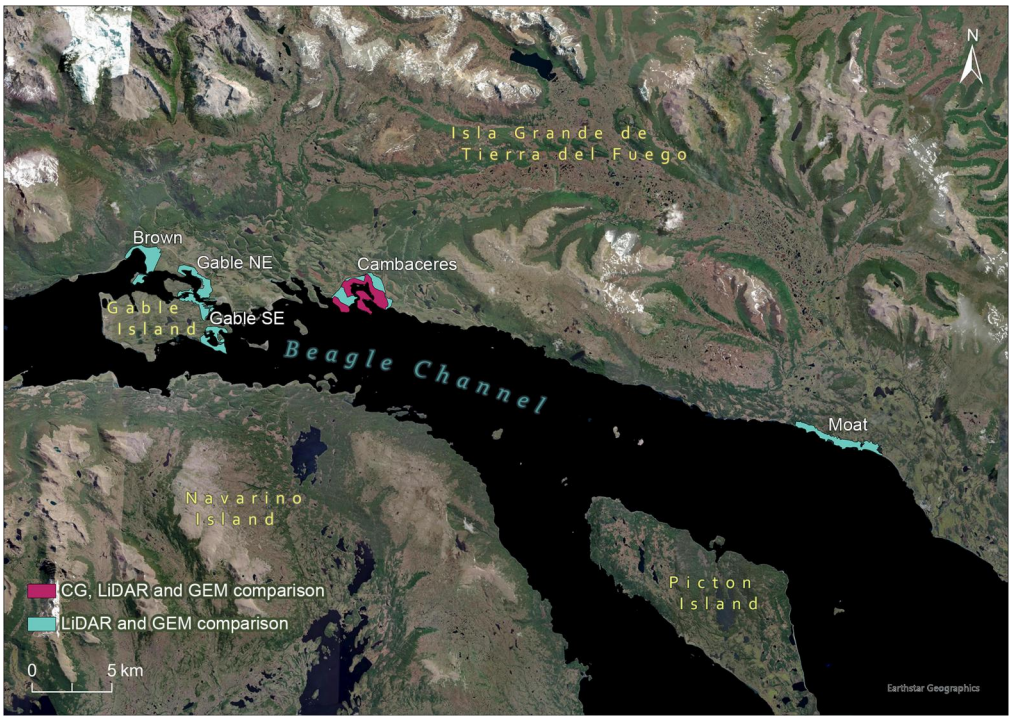


Figure 7. Location of the Cambaceres ground survey (~3 km^2) and UAV LiDAR survey (~12 km^2) areas used in the comparative study. Note that the entire ground survey area was included in the LiDAR survey area. Source: Esri, Maxar, Earthstar Geographics, and the GIS User Community. Illustration: Jo Sindre P. Eidshaug.

areas west of Point Divide and False Cape Horn lack archaeological evidence and the openly available satellite imagery from this region typically has a spatial resolution of 10–30 m (i.e., Google Earth images sourced from Landsat and Copernicus), which is too low for our purpose. Although feature morphology and color signatures can also impact identification (Luo et al. 2018; Thuestad et al. 2021), a spatial resolution of <1 m is usually warranted for visual identification of small features like shell middens (see Beck et al. 2007).

Data collection and processing

Cambaceres ground survey (CG)

Field data were collected during thorough ground surveys based on field walking and surface observations (Bjerck, Zangrando, et al. 2016). Ambiguous features were controlled by cutting the sod with a spade to search for midden material (i.e., dark soils containing charcoal, ashes, shells, bones, artifacts, and burned rocks). Verified middens were recorded as point features with a Garmin eTrex or Garmin Montana 650 with an accuracy estimate ranging between 3 and 5 m in open areas and between 15 and 20 m in wooded areas. Note that midden visibility was severely increased during the CG survey because it coincided with intensive cattle-grazing (Bjerck, Zangrando, et al. 2016, 25).



Figure 8. The GEM survey area covered approximately 3000 km of coastline in southern Tierra del Fuego, from the southern coast of Isla Grande de Tierra del Fuego (Point Divide–Aguirre Bay) and including most of the Cape Horn archipelago. Urbanized areas such as Ushuaia and Puerto Williams were excluded from the surveys due to significant surface modifications. Source: Esri, Maxar, Earthstar Geographics, and the GIS User Community. Illustration: Jo Sindre P. Eidshaug.

UAV LiDAR survey (LiDAR)

Data were collected in 2022 using a Riegl miniVUX-3 UAV Lidar sensor with an Applanix APX-20 UAV GNSS/IMU unit mounted to a DJI Matrice 600 Pro drone (Risbøl et al. 2023). The data were collected in the autumn, before proper defoliation. Maximizing coverage, flight altitude was 107 m above the ground, flight speed 10 m/s, and the drone programmed to follow a line pattern. We used a Carlton BRx7 receiver as a base station and added GNSS corrections during post-processing in Applanix POSPac UAV (v.8.7.) software. Control points were not used. The raw data were further processed in Riegl's RiProcess (v.1.9.) software. Riegl filtering algorithms were used to classify ground and nonground (vegetation) points. Point clouds with average ground point densities ranging from 37 to 66 points per m^2 (pts/m^2) were exported in LAS format (Table 2). Digital elevation models (DEMs) with a resolution of 0.1 m were derived from the LAS files and used for visualization modeling in the Relief Visualization Toolbox (RVT, v.2.2.1.) (Kokalj and Somrak 2019; Zakšek, Oštir, and Kokalj 2011) and ArcGIS Pro (v.3.2.). We used the following visualization techniques to identify shell middens on LiDAR images: local relief models (Hesse 2010), sky-view factor (Zakšek, Oštir, and Kokalj 2011), negative openness (Doneus 2013), local dominance (Hesse 2016), slope, and hill-shade. Quick Terrain Modeler (QTM, v.8.3.) software was used to

support interpretations. All LiDAR identifications were plotted as point features in ArcGIS Pro.

Google Earth desktop survey, supplemented by satellite imagery from ESRI and Microsoft Bing (GEM)

Google Earth images were interpreted by visual desk-based inspection, using Google Earth Pro (v.7.3.6.). The survey covered approximately 3000 km of coastline and included a full kilometer inland in areas north of 55°6′00″ S (Figure 8). The survey concluded in November 2023 and included use of Google Earth's archived imagery to support interpretations (Table 3). Given the notable variations in the quality of Google Earth images (Figure 9), satellite imagery available from ESRI and Microsoft Bing was included in the survey (Table 3). Images in ESRI and Microsoft Bing's repositories had higher resolution and/or quality in southern and eastern parts of the study area, and supplemented interpretations of archaeological features in other areas. All potential shell midden identifications (i.e., ring-shaped middens) were plotted in Google Earth and exported in KML format for conversion to shapefiles and further identification (ESRI and Microsoft Bing) and analysis in ArcGIS Pro.

Comparative analysis

To estimate confidence in GEM identifications of ring-shaped middens, we compared results from the CG, LiDAR, and GEM surveys. The dataset with the highest confidence in each comparison was used as reference data (see Table 1). Only features interpreted as ring-shaped middens from the CG and LiDAR records were used in the comparison. Given that GPS accuracy reached 15–20 m during the CG survey (Bjerck, Zangrando, et al. 2016, 25), we allowed a 20 m offset between LiDAR/GEM and CG coordinates. Based on reported variations in positional accuracy of different image subsets provided by Google Earth (e.g., Benker, Langford, and Pavlis 2011; Paredes-Hernández et al. 2013; Pulighe, Baiocchi, and Lupia 2016), we permitted 10 m offset between GEM and LiDAR coordinates. These offset values also account for potential deviations in the manual plotting of features in the respective datasets.

In the first set of comparisons, the dataset with the highest confidence was used as the source (i.e., CG or LiDAR). In this way, we could quantify identifications and omissions of middens recorded in a dataset with higher confidence (reference data). When the CG survey was the reference, all omissions were assumed to represent false negatives. To deal with GPS inaccuracy and potential offsets between datasets, we used a

Table 2. UAV LiDAR survey area, point spacing, and point densities (points per m^2).

Name (subarea)	Area (km^2)	Point spacing (m)	Point density (pts/m^2)	Ground point density (pts/m^2)
Brown	1.6	0.12	73	41
Cambaceres	4.7	0.10	105	66
Gable NE	2.4	0.12	70	41
Gable SE	1.2	0.11	78	37
Moat	2.3	0.11	85	45
Average	12.2	0.12	64	51

The bottom row provides average values for all fields except area, for which the total value is entered. Note that the UAV LiDAR survey area in Cambaceres is larger than the Cambaceres ground survey area (see Figure 7).

Table 3. Open access satellite images used in the study.

Image	Region	Source	Date(s) of acquisition	Resolution (m)
Google Earth	Cape Horn archipelago	CNES/Airbus	02.10.2016, 20.01.2021	
		Maxar	25.03.2003, 23.01.2011, 03.11.2011, 29.12.2014, 27.08.2021, 28.10.2021, 22.08.2022	
	Hoste Island	CNES/Airbus	06.02.2015, 07.10.2016, 25.10.2018	
		Maxar	07.10.2011, 13.03.2012, 18.04.2013, 03.01.2015, 23.10.2015, 31.10.2018, 05.04.2019, 14.04.2019, 10.03.2021, 21.02.2022, 22.08.2022	
	Isla Grande de Tierra del Fuego	Airbus	18.10.2023, 20.10.2023, 28.10.2023	
		CNES/Airbus	15.02.2014, 04.02.2015, 02.03.2016, 07.10.2016, 25.11.2018, 07.12.2018, 19.12.2018, 04.02.2019, 05.02.2019, 08.02.2020, 15.10.2020, 09.11.2020, 15.11.2020, 10.02.2021, 27.02.2021, 02.03.2021, 20.01.2022, 09.10.2022, 13.11.2022, 28.01.2023	
		Maxar	11.10.2004, 08.09.2005, 17.10.2006, 14.03.2013, 04.02.2015, 01.03.2020, 21.02.2022, 25.12.2022	
	Navarino Island	Airbus	18.10.2023	
		CNES/Airbus	14.02.2014, 06.02.2015, 02.03.2016, 07.10.2016, 26.11.2016, 08.11.2017, 07.03.2018, 25.10.2018, 25.11.2018, 07.12.2018, 04.02.2019, 08.02.2020, 15.10.2020, 10.02.2021	
		Maxar	27.03.2004, 09.02.2005, 23.01.2011, 31.10.2018, 28.10.2021, 21.02.2022	
	Picton, Lennox, and Nueva islands	Airbus	18.10.2023	
		CNES/Airbus	02.03.2016, 04.02.2019	
		Maxar	09.02.2005, 27.12.2009, 28.10.2021	
ESRI	Cape Horn archipelago	Maxar	29.12.2014, 03.01.2015, 06.11.2017, 03.12.2017, 11.01.2019, 28.10.2021, 10.01.2023	0.46–0.5
	Hoste Island	Maxar	03.01.2015, 26.10.2018, 14.03.2019, 08.02.2020, 03.03.2020, 22.11.2020, 31.10.2021, 04.02.2022, 04.03.2022, 11.05.2022, 28.01.2023, 09.02.2023, 21.02.2023	0.31–0.5
	Isla Grande de Tierra del Fuego	Maxar	11.08.2017, 31.12.2018, 11.01.2020, 10.10.2020, 09.11.2020, 21.01.2021, 03.03.2021, 03.10.2021, 28.10.2021, 30.10.2021, 31.10.2021, 14.12.2021, 04.02.2022, 21.02.2022, 25.11.2022, 14.12.2022, 07.01.2023, 09.02.2023, 28.02.2023	0.31–0.5
	Navarino Island	Maxar	11.01.2020, 03.10.2021, 30.10.2021, 31.10.2018, 08.02.2020, 03.03.2020, 15.03.2020, 06.11.2020, 02.01.2021, 10.10.2022, 09.02.2023, 21.02.2023, 28.02.2023	0.31–0.5
	Picton, Lennox, and Nueva islands	Maxar	22.01.2015, 15.10.2015, 10.11.2017, 01.03.2021, 28.10.2021, 21.02.2022, 09.02.2023	0.31–0.5

(*continued*)

Table 3. Continued.

Image	Region	Source	Date(s) of acquisition	Resolution (m)
Microsoft Bing	Cape Horn archipelago	CNES/Airbus, Maxar, TomTom	22.02.2008–30.01.2016	
	Hoste Island	CNES/Airbus, Maxar, TomTom	23.11.2008–25.02.2016	
	Isla Grande de Tierra del Fuego	CNES/Airbus, Maxar, TomTom	21.01.2004–25.02.2016	
	Navarino Island	CNES/Airbus, Maxar, TomTom	23.11.2008–25.02.2016	
	Picton, Lennox, and Nueva islands	CNES/Airbus, Maxar, TomTom	31.12.2009–27.01.2016	

Image information is lacking from Google Earth (resolution) and Microsoft Bing (exact source and date of acquisition, and resolution).



Figure 9. Notable variations in resolution were observed on Google Earth images—ranging from high-resolution images in the central part of the Beagle Channel to poor and inadequate resolution in certain areas in the southern and eastern parts of the survey area. All images at same scale. Source: Google Earth, CNES, Airbus, and Maxar Technologies. Illustration: Jo Sindre P. Eidshaug.

methodology described in Risbøl et al. (2023, 542–3): to compare the CG record and GEM identifications, we applied the *CG* coordinates (i.e., values from the source, as center-points for generating dissolved buffer polygons with 20 m radiuses equal to maximum GPS offset value) and then calculated the differences between CG and GEM point frequencies within each polygon. Subsequently, we summarized LiDAR points within the same polygons to recalculate the difference between the CG survey record and LiDAR identifications.[4] For comparing LiDAR and GEM identifications, we repeated the steps described above, applying 10 m buffer polygons centered at LiDAR coordinates.

In the second set of comparisons, the steps of the method of buffer polygon comparison described above were repeated using the dataset with the lowest confidence as the

source (i.e., LiDAR or GEM). In this way, we could quantify anomalies in a dataset with lower confidence without matches in the reference data (i.e., a dataset with higher confidence). These unverified anomalies can include: (1) false positives (i.e., LiDAR or GEM anomalies mistakenly identified as middens); and (2) identifications of new features (i.e., ring-shaped middens not recorded in the dataset with higher confidence). Given the expectation that no new features were identified in GEM data in areas where they overlap with CG and/or LiDAR data, false positives in the GEM data were assumed to be equal to unverified anomalies.

However, for the LiDAR data, it was necessary to consider that the unverified anomalies contained new identifications. Based on the results of post-LiDAR survey field verification of a small sample of 26 unverified anomalies in Cambaceres,[5] Risbøl et al. (2023, 548) suggest that about 50 new identifications of ring-shaped middens were included among the 241 unverified anomalies (27% of the 905 LiDAR included in the ring-shaped midden category). This gave a conservative estimate of 20% new identifications and 80% false positives among the unverified anomalies. However, the proportion of false positives among the unverified anomalies was expected to be slightly lower in this study (perhaps two out of three) because 140 LiDAR anomalies from Risbøl et al. have been excluded in this study (see note 4).

The comparison of LiDAR and GEM data was complicated because the dataset with the highest confidence also contained false negatives and false positives. As such, to assess the effect of false negatives and false positives on the results, we used the following equation to model the GEM detection rate in the LiDAR survey area:

$$\frac{GEM\ \ count}{(LiDAR\ \ count + LiDAR\ \ false\ \ negatives - LiDAR\ \ false\ \ positives)}$$

The estimated number of false negatives and false positives for the LiDAR survey area were found by multiplying the rates found in the comparison of LiDAR and CG data. Provided that we could not determine with any confidence the rate of false positives in the LiDAR data, we modeled two scenarios: one with 50% and one with 80% false positives among the unverified anomalies. The estimated percentage of false positives among all LiDAR identifications was then found by dividing the number of false positives with the total LiDAR count from Cambaceres. Finally, LiDAR and GEM datasets were compared at cluster level to determine dimensions of identified and omitted clusters. A cluster was defined as an agglomeration of ring-shaped middens (one ring-shaped midden equals one [point] feature), where 20 m was set as the maximum distance between point features included in a cluster (i.e., roughly the center-points of the middens). Based on midden counts from the LiDAR dataset, the following four cluster categories were defined:

- Very large clusters: $\geq$100 middens
- Large clusters: 40–99 middens
- Medium clusters: 15–39 middens
- Small clusters: 1–14 middens

Clusters generated from the LiDAR and GEM datasets were compared manually.

Results

Comparison of GEM, LiDAR, and CG datasets

The CG record of 802 ring-shaped middens yielded 631 matches with LiDAR identifications[6] and 406 matches with GEM identifications. This is equivalent to a detection rate of 79% for LiDAR and 51% for GEM (Figure 10).

The comparison of LiDAR and GEM identifications provided a similar GEM detection rate of 53% ($n = 863$) based on 1625 LiDAR identifications. There was some variation in GEM matches with LiDAR identifications at the subarea level (Figure 10): Gable Island SE had the highest detection rate, with 69% of the ring-shaped middens identified. This area hosts a very large cluster consisting of 200 ring-shaped middens identified on LiDAR images—of which 159 were identified on GEM images. The percentage of false positives among GEM identifications appears to be low (5–6%), even if we assume that no new features were identified on GEM imagery (Table 4).

As noted above (Methods), the direct comparison of LiDAR and GEM identifications did not account for false negatives and false positives among LiDAR identifications. False negatives (assumed to be equal to LiDAR omissions of middens recorded during the CG survey) totaled 21% for Cambaceres (Figure 10) while false positives were estimated to 9–14% (Table 4). Multiplied by the 1625 LiDAR identifications in the UAV LiDAR survey area (Figure 10), we found the estimated numbers in this area of false negatives to be 340 (0.21×1625) and false positives to be between 146 (0.09×1625) and 227 (0.14×1625). Given the low percentage of false positives in the GEM data (Table 4), the modeled GEM detection rate was given by entering these numbers into the following equations (see Methods):

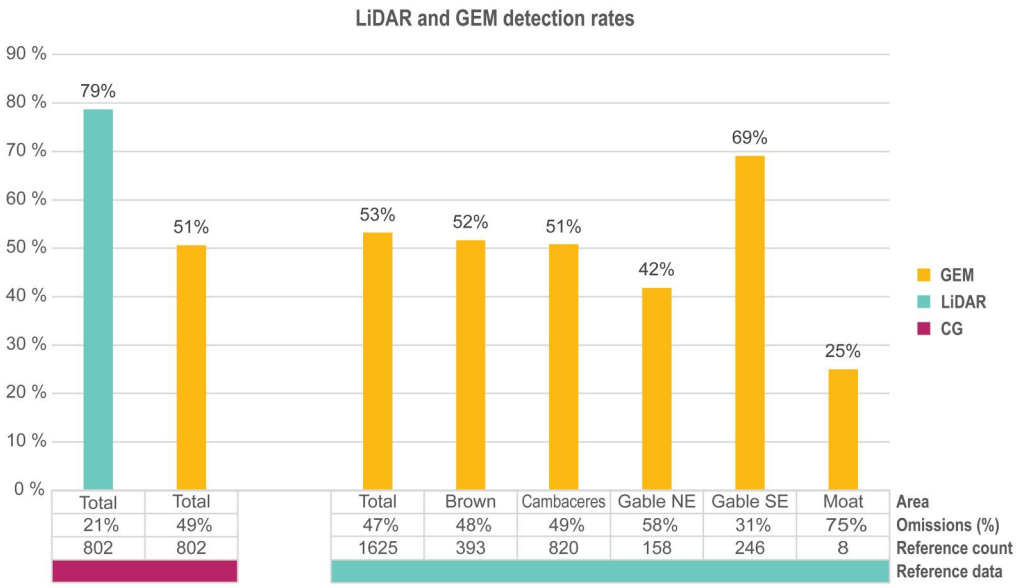


Figure 10. Results from comparisons of GEM, LiDAR, and CG records, showing GEM- and LiDAR-based identifications and omissions of ring-shaped middens recorded in the datasets with higher confidence (reference data). Illustration: Jo Sindre P. Eidshaug.

Table 4. Proportions of verified and unverified GEM and LiDAR anomalies when compared to reference data with higher confidence (CG and LiDAR).

Dataset	Anomalies	Verifications	Unverified anomalies		False positives estimate	
	Count	%	Count	%	%	Reference data
LiDAR	763	82%	134	18%	9–14%	CG
GEM	439	95%	24	5%	5%	CG
GEM	922	94%	57	6%	6%	LiDAR

While the unverified anomalies from the LiDAR survey include a certain proportion of new identifications in addition to false positives (see Risbøl et al. 2023), we expect no new identifications from the GEM survey within the comparative study area. Hence, the proportions of unverified GEM anomalies provide estimates of false positives among GEM identifications.

$$\frac{863}{(1625+340-146)}=0.48 \text{ and } \frac{863}{(1625+340-227)}=0.50$$

Thus, given that the modeled rate (48–50%) was only slightly lower than the results from the direct comparisons (51–53%), the average GEM detection rate appeared to be around 50%.

GEM- and LiDAR-identified clusters

Ring-shaped middens. The average proportions of ring-shaped middens identified in very large (76%) and large clusters (69%) (Figure 11) were substantially higher than the average GEM detection rate. For medium and small clusters, these figures were 56% and 31%, respectively. The aggregated average proportion of GEM identifications on medium to very large clusters is 67%. This value, 0.667, was used as a LiDAR–GEM ratio to define proportional cluster categories for GEM identifications (see Table 5).

Clusters. Thirty-nine of the 62 clusters identified during the GEM survey were matched with the correct category, using a LiDAR–GEM ratio of 0.667. Most clusters (i.e., 89%) with 15 or more ring-shaped middens (i.e., very large, large, and medium clusters) were identified on GEM imagery (Table 5). The two very large clusters from the LiDAR survey were correctly identified on GEM images, and five of six clusters were correctly identified as large (the omitted cluster is covered by trees). Seventeen of 19 medium clusters were identified in GEM data, but only 10 were correctly identified. This means that 63% of the clusters with 15 or more ring-shaped middens (based on LiDAR data) were identified in the correct category during the GEM survey. The total number of GEM omissions is high due to relatively few identifications of small clusters: only 30 of 109 were identified of which 22 were identified correctly.

GEM survey

Covering almost 3000 km of coastline, altogether 6647 potential ring-shaped middens were identified during the GEM survey, distributed over 574 shell midden clusters (Figures 12 and 13). Twelve of these are very large clusters while 389 have fewer than 10 identifications (i.e., small clusters). The largest cluster comprises 227 potential middens and is located on the northern coast of the Beagle Channel, *vis-à-vis* Puerto

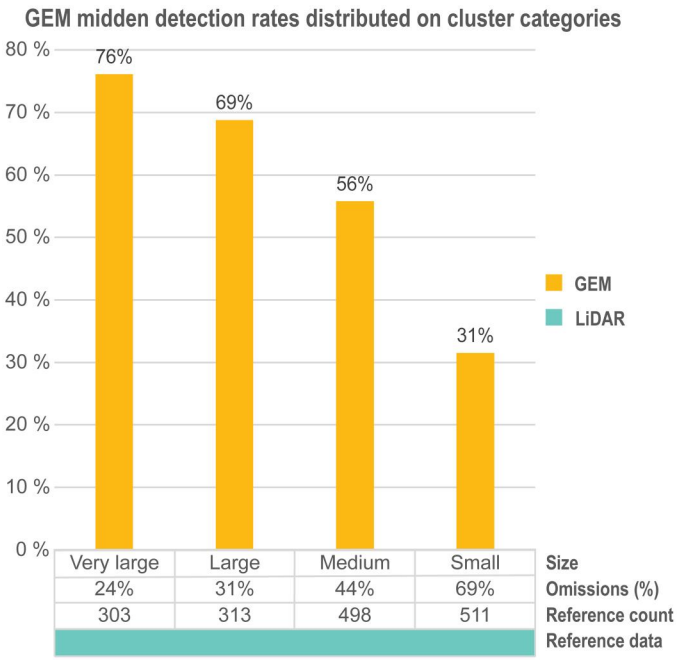


Figure 11. Comparison of LiDAR and GEM identifications of ring-shaped middens distributed on cluster categories. The table shows that the number of ring-shaped middens identified on very large, large, and even medium clusters are above the average GEM detection rate while a substantial number of shell middens from small clusters are omitted. Illustration: Jo Sindre P. Eidshaug.

Table 5. Comparisons of clusters identified on LiDAR and Google Earth images.

Description	Very large	Large	Medium	Small	Total
LiDAR clusters	2	6	19	109	136
LiDAR clusters identified in GEM data	2	5	17	30	54
% LiDAR clusters identified in GEM data	100%	83%	89%	28%	40%
GEM and LiDAR cluster categories matched	2	5	10	22	39
% GEM and LiDAR cluster categories matched	100%	83%	53%	20%	29%
GEM clusters with false category	0	3	6	14	23

The table shows that most clusters with 15 or more ring-shaped middens were identified on GEM imagery (i.e., without respect to the actual proportions of features identified on each site). However, smaller proportions were identified as the correct category if we assume the identification of 66.7% of the features on GEM imagery.

Mejillones on Navarino Island. Almost all GEM identifications were in the Beagle and Murray channels.

The highest density of GEM identifications is concentrated in a 16-km run in the central part of the Beagle Channel (Figure 12). This area (hereafter "the Gable Island area") consists of approximately 150 km of coastline, and includes Gable Island and Cambaceres on Isla Grande and the opposite coastal territories of Navarino Island. Almost half (45%) of the identified middens ($n = 3007$) and more than half of the clusters with 27 or more middens are found here (Figure 13): eight of 12 very large clusters and 24 of 41 large clusters. Very high densities are also found on the north-western coast of Navarino Island, *vis-à-vis* Ushuaia,[7] and high densities occur on Isla Grande, somewhat east of Ushuaia—mostly due to the location of the largest cluster along this stretch (Figure 12).

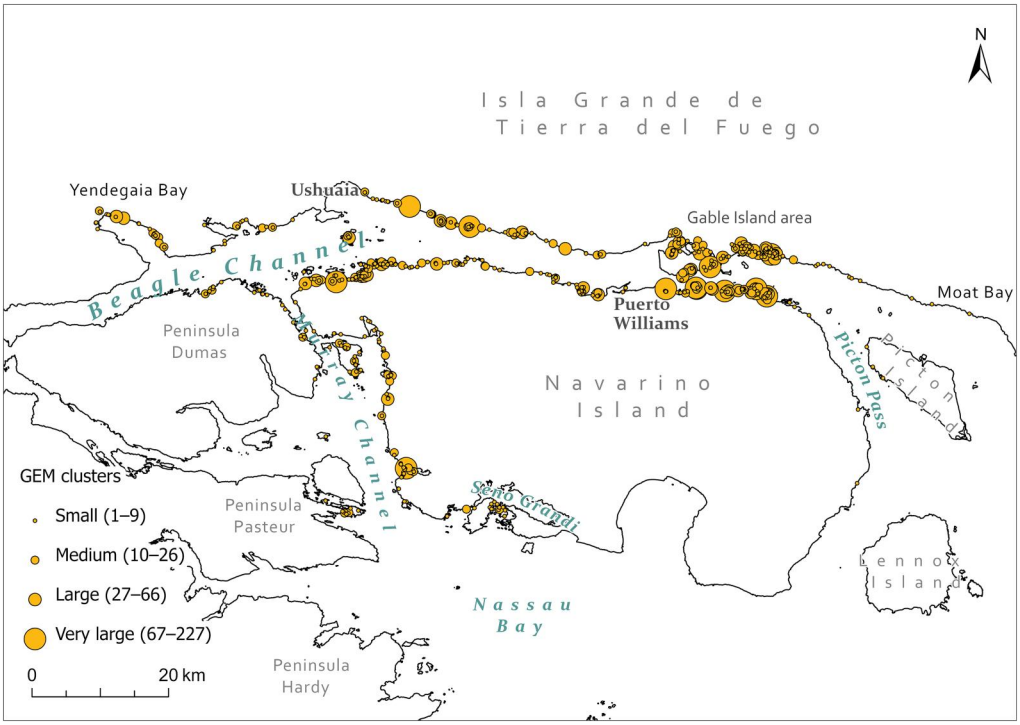


Figure 12. Settlements identified during the GEM survey, showing an uneven distribution across southern Tierra del Fuego. Almost all 6647 identifications were located in sheltered areas, in the central part of the Beagle Channel and in the neighboring Murray Channel. Interestingly, a clear concentration consisting of 3007 ring-shaped middens was found in the Gable Island area. The maximum distance between middens included in a cluster is 20 m, measured between point features (i.e., roughly the center-points). Illustration: Jo Sindre P. Eidshaug.

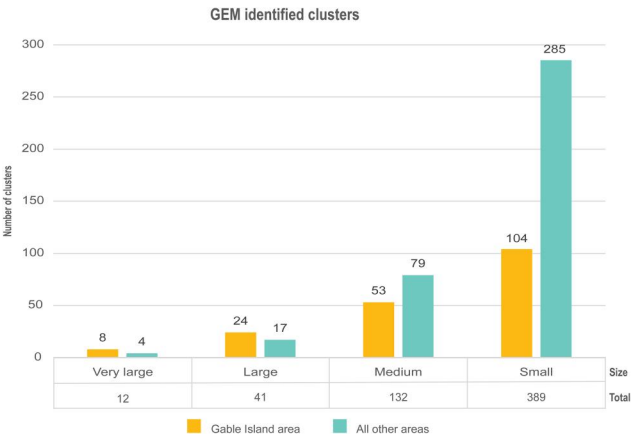


Figure 13. Clusters of ring-shaped shell middens identified during the GEM survey, showing that more than half of the very large and large clusters are located in the Gable Island area. Total figures are displayed in the table beneath the columns. Illustration: Jo Sindre P. Eidshaug.

Discussion

Confidence in GEM imagery from Tierra Del Fuego

The results from the evaluation of confidence in the GEM survey are convincing. We can plausibly assume to identify half of the ring-shaped middens in southern Tierra del Fuego based on desktop visual interpretation of satellite imagery accessed on Google Earth, ESRI, and Microsoft Bing. Furthermore, we are reasonably confident that we can identify almost nine out of 10 clusters consisting of 15 or more ring-shaped middens, and that we can match around two-thirds of the very large, large, and medium clusters with the correct category. The size of a cluster is an important indicator of settlement impact and occupation intensity because of the way in which midden material accumulated in southern Tierra del Fuego. Archaeological excavations indicate that shell midden formations resulted from repeated occupations interrupted by short- and long-term periods of inactivity (Piana and Orquera 2010; Zangrando 2018). In other words, larger sites are agglomerations of smaller sites. Given this widespread regularity in reusing the same places in the landscape, identifying larger clusters on GEM imagery is imperative for assessing distribution and trends pertaining to the ring-shaped shell midden tradition. Moreover, this diminishes the impact of the caveat that relatively few small clusters are identified on GEM imagery. Thus, even though we cannot identify the full inventory of sites, we find these figures appropriate for macro-regional studies of coastal settlement structure.

Vegetation and poor resolution are key challenges for identifying archaeological features on satellite imagery. The large cluster that was omitted during the GEM survey consists of rather small (low) ring-shaped middens located in an area with shrubs while the two omitted medium clusters are in wooded areas. While these three clusters were identified with LiDAR, dense vegetation is also a known factor that can reduce visibility of archaeological features on LiDAR images (Doneus, Banaszek, and Verhoeven 2022; Masini et al. 2018; Sadr 2016). The main factors impacting LiDAR identifications in Cambaceres were midden shape, size, location, and vegetation (Risbøl et al. 2023, 548–50): concave (dome-shaped) and/or small (dome- and ring-shaped) middens located outside clusters and/or in areas with denser vegetation away from the shore were often not visible in the LiDAR data.

The factors that affected identification on LiDAR images apply to GEM images to a greater extent (Figure 14). Optical sensors cannot "see" what is hidden by vegetation cover or other physical obstacles while feature characteristics, including size (of the midden or cluster) and morphological regularity, certainly influence how easily features are perceived in image data (e.g., Thuestad et al. 2021). Ring-shaped middens consist of both convex and concave shapes—and the more pronounced the latter, the easier they are to identify. The extent to which archaeological features are visible or not in the imagery not only depends strongly on vegetation (and cloud) cover, but also vegetation type, seasonal variation, soil type, topography, and land use (Beck et al. 2007; Luo et al. 2018)—the latter of which often is anthropogenically contingent (e.g., see Erlandson et al. 2019). Multi-temporal coverage can alleviate the impact of some of these factors and, when possible, inspecting multiple images in the historical archives of Google Earth and ESRI to identify the most optimal conditions was imperative for the result.

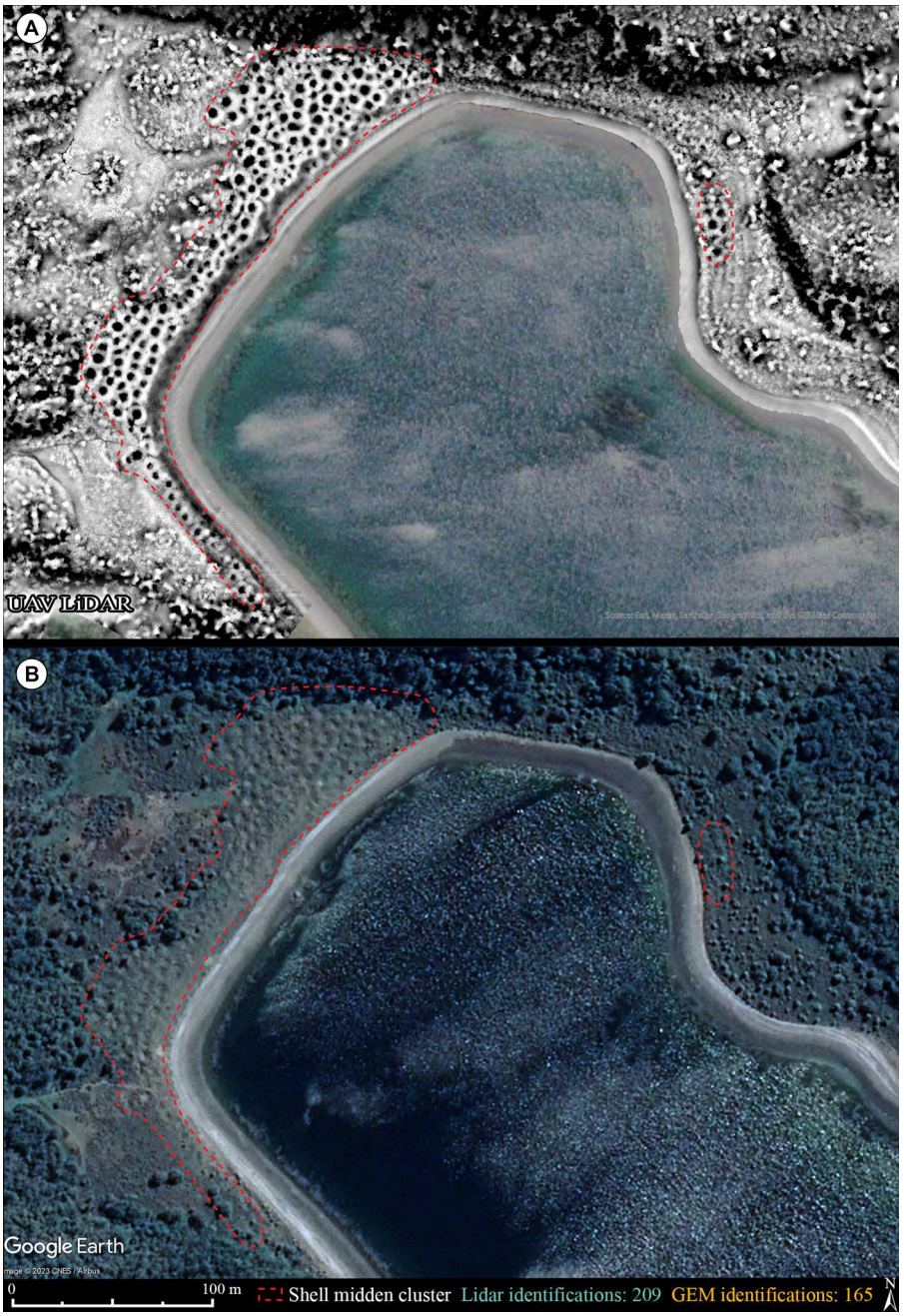


Figure 14. An example of visibility of ring-shaped middens on: (A) LiDAR images (applying sky-view factor as a visualization technique, see Kokalj and Somrak (2019) and Zakšek, Oštir, and Kokalj (2011)); and (B) Google Earth images (CNES/Airbus, dated February 4 2019). More recent images are available from Google Earth, but the middens were most visible on the current image from 2019. The clusters, indicated by red dotted lines, are located on Gable Island and shown in Figure 4B. Illustration: Jo Sindre P. Eidshaug.

And in many cases, identification was aided by pronounced differences in the ground vegetation, especially changes in green tones, in and around middens (see Zangrando 2018; see below). Apart from omissions of middens covered by vegetation, very few small clusters were identified in the study (Figure 11), presumably because the archaeological signature was invisible or too insignificant or undeterminable against the "background." In the Cambaceres Bay area, ring-shaped middens are generally larger—and vegetation sparser—closer to the shore (Bjerck, Zangrando, et al. 2016, 75). Figure 15 illustrates the effects of vegetation and midden size on interpretations of LiDAR and GEM data: ring-shaped middens in these datasets are concentrated to areas close to the shore, below the marine ridge (5 m a.s.l.).

Nonetheless, the results for Tierra del Fuego are remarkably persuasive, particularly since the GEM imagery lacks spectral information and many qualities associated with LiDAR, including its high resolution (Table 2), *z*-values (required in relief visualizations), precision, and ability to penetrate vegetation. Whereas we lose some information due to qualitative differences, we certainly gain much in cost-effectiveness and extensiveness of coverage with GEM data (Sadr 2016)—especially because most ring-shaped middens are located in the more open, coastal areas (Barceló, Piana, and Martinioni 2002; Risbøl et al. 2023).

Distribution of ring-shaped shell middens

The GEM survey indicates that the distribution of ring-shaped middens is strongly concentrated in the Beagle and Murray channels (Figure 12). While it cannot be concluded that this type of structure is completely absent outside those areas based on this survey,

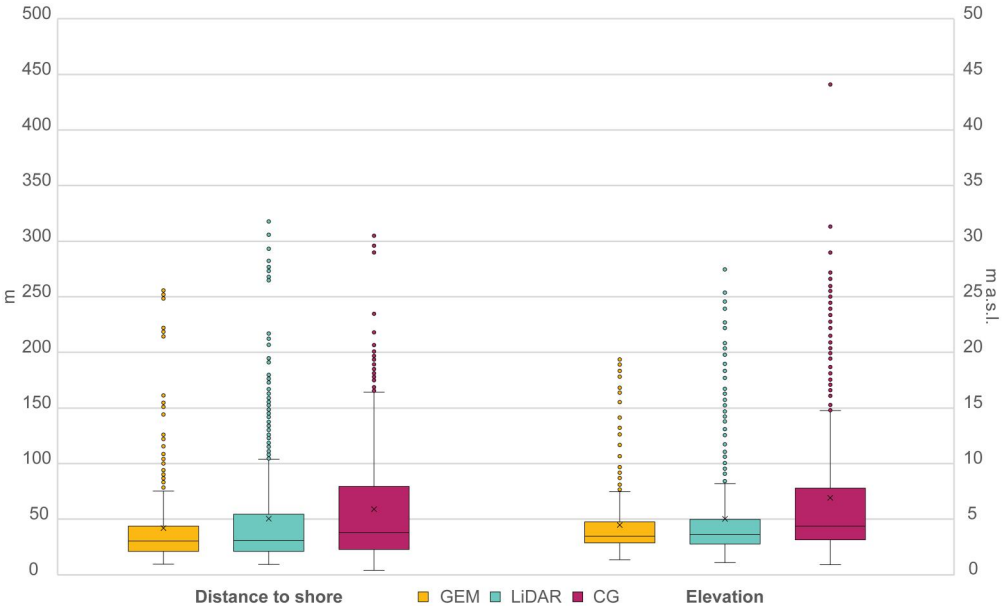


Figure 15. Distance to shore and elevation of ring-shaped middens recorded during the three surveys. Elevation values were extracted from the DEM generated from the LiDAR data. Illustration: Jo Sindre P. Eidshaug.

such a distribution seems well supported by archaeological data. The southernmost GEM identifications were located around the southern mouth of the Murray Channel and on the southwestern coast of Navarino Island (Seno Grandi). Archaeological investigations have identified significant differences between this region and the Cape Horn archipelago (Legoupil 1993–1994). Whereas ring-shaped middens are common in Seno Grandi, most shell middens in the Cape Horn region are small, isolated mounds (domes)—typically situated at the edge of the stunted forest in small, sheltered coves (Legoupil 1993–1994).

The easternmost GEM identifications are found somewhat west of Moat Bay. However, notably few were located east of Cambaceres, where the Beagle Channel is more open and exposed. Archaeological information suggests a similar pattern: few ring-shaped middens were discovered in the thoroughly surveyed Moat area (Zangrando 2010), where shell midden mounds (domes) predominate (Zangrando et al. 2014). Further east, in Peninsula Mitre, the recorded middens are generally small and shaped as mounds, if not preserved only as thin shell-bearing strata (Vázquez et al. 2011).

In the west, GEM identifications indicate a boundary by Yendegaia Bay. Here, many ring-shaped middens have been recorded during archaeological surveys (Gallardo et al. 2023, 535–6).[8] Unfortunately, data from the far more exposed region further west are scant due to few investigations (Borrero, Morello, and San Román 2020, 51; San Román et al. 2016, 170).

There is a remarkable temporal stability with respect to the eastern and southern boundaries of the ring-shaped midden tradition. Radiocarbon dates from excavated ring-shaped middens around the southern (Grandi 1) and eastern (Imiwaia I) boundaries are both among the oldest in southern Tierra del Fuego (Orquera, Legoupil, and Piana 2011; Orquera and Piana 2020).

Exploring large-scale trends

The GEM survey demonstrates that shell middens are not evenly distributed across the Fuegian archipelago. This is underscored by the striking concentration of ring-shaped middens in the Gable Island area (Figure 12), which amounts to 3007 GEM identifications (45%) within an area consisting of 150 km of coastline. This area also hosts two-thirds of the very large clusters (Figure 13)—those consisting of 67 or more GEM-identified middens—typically situated in eastern-facing, sheltered bays (the major winds come from the west). The coastal configuration of the Gable Island area is characterized by a drumlin field interspersed by the sea, creating a mosaic of land and sea, including ample areas with shallow waters. The curving coastlines have many good landing places for boats and provide extensive areas of accessible intertidal beach (with shell beds and other benefits) within close proximity of the sites. Overall, this sheltered area of the Beagle Channel stands out as well suited for the elaboration of marine lifestyles. Curiously, the Gable Island area is also located near the historical boundaries between the Yagan and Selk'nam/Haush territories, and between the distributions of the Eastern and Central dialects (Figure 2).

Bjerck (2009) distinguishes between land-based maritime relations (littoral relations) and sea-based maritime relations (marine relations) (see also Lyman 1991, 76; Orquera and Piana 1999, 96). While littoral and marine relations both include foraging in the littoral zone, the latter additionally encompasses widespread use of boats, which enables a wide variety of activities on the open sea, including fishing, hunting, and traveling (Bjerck 2009; Bjerck and Zangrando 2016). In a wide sense, these relations are encountered in Fuegian ethnography—the Selk'nam and Haush representing littoral relations, and the Yagan marine relations. Although the distribution of ring-shaped middens does not correspond with the territorial extents of any of these groups, the highest densities are concentrated in areas that were inhabited by marine foragers during the Holocene until historical times (i.e., the Beagle and Murray channels; Figure 12) (Orquera and Piana 1999). Still, ring-shaped middens have not been recorded in many sectors that these societies occupied during the late Holocene (e.g., Cape Horn archipelago, Hardy Peninsula on Hoste Island, Nassau Bay, Picton Island, Lennox Island, and Nueva Island).

Conversely, shell middens with dome-shaped formations have a wider distribution in the Fuegian archipelago. This is certainly the case along the southern coast of Isla Grande: domes are the dominant features from Moat toward the eastern end of the Fuegian region. Furthermore, dome-shaped structures are also frequent in areas with high densities of ring-shaped middens (for instance, Bjerck, Zangrando, et al. (2016, Table 2) identified 432 domes among the 1237 shell middens recorded in the Cambaceres surveys). Notably, no significant differences in composition between dome- and ring-shaped deposits have been identified at the microscale structure. Extensive excavations of both midden types show similarities in technological composition and in exploitation patterns of an important diversity of animal resources (Alunni, Tivoli, and Zangrando 2020; Estevez et al. 2001; Orquera and Piana 1996; Tivoli and Zangrando 2011). Moreover, information derived from technological and zooarchaeological studies indicate that the composition of both types of deposits result from multiple activities (Orquera and Piana 1999).

However, there is a striking trend that crystallizes through the vast number of identifications of ring-shaped middens. Observing the data from a landscape perspective, the sheltered channels present evidence of a considerably higher occupation intensity than the remainder of the Fuegian archipelago (Figure 12). Why are the clusters of ring-shaped middens concentrated to the Beagle and Murray channels? It has been argued that such sheltered waters between land and open oceans (i.e., archipelagic seascapes consisting of skerries, fjords, channels, islands, islets, etc.) provide ideal conditions for marine exploitation (Orquera and Piana 1999)—including the development of marine relations (Bjerck 2009).

In southern Tierra del Fuego, the use of boats is evident from the emergence of shell middens ca. 7000 cal BP (Orquera and Piana 2009), and recent discoveries on Bridges Islands (Beagle Channel) may further push the antiquity of seaborne vessels in the region (Tivoli et al. 2022). It is well-documented in historical sources that bark canoes were of paramount importance for the Yagan (Figure 16) (Gusinde 1937, 611–8; Orquera and Piana 2015, 231–59). Moreover, the centrality of seaborne mobility in Yagan lifeways is underscored by linguistic information: the word canoe was used in



Figure 16. Yagan bark canoe in New Year Sound (Lajarte Channel). Photo: Jean Louis Doze and Edmond Payen, 1882–1883.

almost 4% of the English translations of the approximately 22,800 Yagan words enlisted in Reverend Thomas Bridges (1987) late nineteenth century Yagan–English dictionary (Eidshaug et al. 2024).

As should be clear from previous sections, we do not intend to set up a dichotomy based on ring- and dome-shaped middens. However, the majority of shell middens—including more than 50 large clusters of ring-shaped middens—are located in sheltered channels that favor marine relations. The same may be true for most dome formations (at least those interspersed with ring-shaped middens and/or located on islands), but not necessarily for the entire widespread distribution of shell midden domes across the eastern part of Isla Grande. While other types of evidence are needed to support the idea that littoral relations were more commonplace in Moat[9] and on Peninsula Mitre, the main point to stress is the marked difference in the occupation intensity near calmer waters compared to more exposed areas.

The striking correlation between the locations of clusters of ring-shaped middens on the one hand, and safe harbors and sheltered sea on the other—as noted in the Cambaceres surveys report (Bjerck, Zangrando, et al. 2016)—appears supported by the current study. Waters and coasts are more exposed almost immediately outside the main distribution of ring-shaped middens (Figure 12). East of the division between the Beagle Channel and the Picton Pass, the bays are larger and more open, and there are fewer landing places for canoes (Figure 17). Weather is even more fierce in the south, closer to Cape Horn. One year it was reported that there were "three hundred days of continuous rain, twenty-five storms, the other days neither fine nor wet" from the short-lived Anglican mission (1888–1892) in the northern part of the archipelago (as quoted in Barclay 1926, 140). Despite regular crossings of Nassau Bay in the late Holocene (Legoupil 1993–1994) and risky ventures to Ildefonso Islands (Bridges 1893)



Figure 17. Overview of the large and open Moat Bay in the more exposed, eastern part of the Beagle Channel. Nueva Island is seen in the background. Photo: Jo Sindre P. Eidshaug.

and across the Le Maire Strait being recorded (Horwitz and Weissel 2011), weather would most certainly affect choices on a daily basis (Bjerck 2021; see Ingold 2007).

Another factor that may have impacted shell midden distributions across the Fuegian archipelago is seasonal patterns. Ethnographic sources indicate that despite their high residential mobility, the Yagan led a relatively sedentary life in the winter (Bridges 1866, 207), accordingly due to the greater diversity of resources during summer (Gusinde 1937, 620). Martial (1888, 196) noted that groups with canoe people spread out during the summer and took refuge in the channels during winter. These observations from the ethnographic record suggest that the channels were occupied more intensively and throughout longer seasonal periods than other areas of the archipelago—which could help explain the high density of shell midden clusters in the Beagle and Murray channels. Preliminary seasonality studies from serial measurements of $\delta^{18}O$ in *Nacella* shells from the Lanashuaia I site (ring-shaped structure), Cambaceres Bay (Colonese et al. 2012), and in Heshkaia 35 (dome-shaped structure), Moat Bay (Pérez, Tessone, and Zangrando 2022), indicate similar seasonal patterns throughout subsequent occupations of those sites.

A somewhat different point of discussion refers to the practice of reuse and the formation of large clusters of ring-shaped middens. Why do certain clusters have huge concentrations of shell middens while they are absent in other places? Concerning this question, local phenomena and conditions seem to have played important roles. Shell midden formation necessarily results in the rearrangement of the conditions in the landscape (Zangrando 2018). As Piana and Orquera (2010) argue, shell middens worked as attractors in the landscape. The continued reuse and gradual accumulation of midden materials made them conspicuous features in the Fuegian seascape. Existing ring-shaped middens provided many favorable conditions, such as ready-made, well-drained, wind-sheltered sites for dwellings.

However, ring-shaped middens also had entrapping effects. Even when periodically unsettled (short-term or long-term hiatuses in archaeological records), they were always "present," attracting, and ready to once again "take on" functions as foundations for dwellings. They take on this function not only because of tradition and reuse, but also as an outcome of a series of micro-environmental processes (Fretheim et al. 2016; Piana and Orquera 2010; Zangrando 2018). Shell accumulations produce high concentrations of $CaCO_3$ (calcium carbonate) in soils, modifying the environmental conditions for ground vegetation. Thus, occupation intensity and shell midden density are also influenced by complex entanglements between humans and nonhumans at the local level. Within such a striated seascape created by clusters of ring-shaped middens—providing the benefits of protection from the wind and substrate drainage—reoccupation would be a more likely choice than establishing a new settlement in any "random" bay.

Conclusions

It is useful to conceive satellite data with multi-temporal coverage and variable spatial resolution as Big Data. It means accepting that data necessarily are fragmentary and fluctuating in terms of resolution, quality, and source, for achieving the benefits of cost-efficient desk-based studies with large spatial extents. However, it also serves as a reminder not to ignore data confidence assessments. Previous ground and UAV LiDAR surveys are examples of smaller datasets with higher confidence that can serve as independent measurements of data quality—and a form of field verification is imperative when using Google Earth and other virtual globes (Luo et al. 2018). Through the case study from Tierra del Fuego, we have aimed to show that approaching fragmentary and messy Google Earth data methodically by use of such small-scale datasets to evaluate data quality can be fruitful.

In this study, we compared satellite imagery accessed on Google Earth (supplemented with imagery from ESRI and Microsoft Bing) at local scales with previous records from a 3 km^2 ground survey and a 12 km^2 UAV LiDAR survey. The results were convincing for studying the distribution of ring-shaped middens in southern Tierra del Fuego, especially given that virtually all clusters with 15 or more ring-shaped middens were identified and two-thirds were identified as the correct category. Not surprisingly, omissions were mostly small clusters of ring-shaped middens (less than 15 middens), located in wooded areas, at higher elevations farther from the coast, and/or consisting of small (low) middens.

Based on interpretations of open-access satellite imagery from 3000 km of coastline, we find that the tradition and cultural practice of creating ring-shaped middens is associated with important variations in occupation intensity between calmer waters and more exposed areas. Marine relations include the use of boats in a wide range of activities on the open sea (sensu Bjerck 2009), and it is suggestive that the distribution of ring-shaped middens is confined to the more sheltered areas in the Beagle and Murray channels. Moreover, almost half of the identified ring-shaped middens were located in the Gable Island area, which consists of bays and coves, channels and narrows, islands, and islets that provide protection from the wind and natural harbors. Ventures past the sheltered homeland were not uncommon, at least not in the summer—and during the

late Holocene. However, they potentially involved greater risk, as the sea is more open and exposed in the areas outside the main distribution of ring-shaped middens.

The case study from Tierra del Fuego shows that the free, open-access satellite imagery that is available from virtual globes like Google Earth can provide a sound empirical basis for studies at a macro-regional scale and thereby contribute to new archaeological insights (see also Bewley et al. 2016; Kennedy and Bishop 2011; Luo et al. 2018; Sadr 2016), as long as the archaeological features can be identified in the data and the quality of the data is evaluated. Obviously, a similar study emphasizing dome-shaped middens in Tierra del Fuego would not be possible due to their poor visibility on Google Earth imagery. To overcome such limitations, other types of remote sensing technologies should be explored. And given that middens modify conditions for ground vegetation, it would be interesting to see studies of these sites based on multi-spectral images in the future (e.g., see Agapiou et al. 2014; Oltean and Abell 2012; Thuestad et al. 2021). However, under favorable conditions where archaeological structures are visible in the data, we are confident that the methodological approach applied here has transfer value to studies of other geographical regions, including coastal and island regions hosting certain types of conspicuous shell middens, and for addressing various archaeological issues—especially regarding trends at the macro-regional scale.

Notes

1. While Google Earth, ESRI, and Microsoft Bing combine satellite and aerial images with higher resolution, only satellite imagery is currently available from southern Tierra del Fuego.
2. The oldest sites are pre-transgressive and consist of lithic assemblages without midden deposits. The shell-bearing layers in Imiwaia I superseded the oldest archaeological context recorded in the Beagle Channel region, dated to ca. 8600 cal BP (Zangrando et al. 2016, 2022).
3. The terms "dwelling" and "dwelling pit" are used in place of ring-shaped midden in the report.
4. New calculations were essential because Risbøl et al. (2023) included structures without visible traces of shell middens (depressions only) in the category "ring-shaped middens." Thus, the LiDAR count reported in this study was reached by excluding 140 of the 905 LiDAR anomalies included in the ring-shaped midden category by Risbøl et al. (2023).
5. Only six of these anomalies are included in the present study, of which two were verified and four disproved as false positives. Thus, these data are far too limited to be conclusive.
6. Occasionally, distinctions between ring- and dome-shaped middens may be subtle, implying that different classifications potentially may have been applied to some middens in the ground and LiDAR surveys (Risbøl et al. 2023, 550). However, the number of features recorded during the Cambaceres survey ($n = 1240$) that were not among the LiDAR identifications in Risbøl et al. (2023, Table 3) only increased by 30 (i.e., about 2%) when shell midden category (ring-shaped and dome) was used as a restraint in the comparison. This strongly suggests that misclassification is not an issue that requires further consideration.
7. Although the city of Ushuaia was excluded from the study because of the significant modern surface modification, it should be noted that *very large* sites also have been recorded here, e.g., on aerial photographs from 1970.
8. Gallardo et al. (2023) apply the terms "pit houses" (sensu Bird 1938) and "semi-subterranean dwellings" instead of ring-shaped middens.
9. Zoological and artefact assemblages from excavations of Late Holocene shell midden mounds in Moat Bay (Heshkaia) thus far imply foraging from the coast (Corbat, Tivoli, and Zangrando 2020; Zangrando et al. 2014).

Acknowledgements

We are indebted to our colleagues and those directly and/or indirectly involved in fieldwork during the Cambaceres surveys and UAV LiDAR survey, particularly Ernesto Piana, Magnar M. Gran, Martín Castro, Adalberto Ferlito, and Juan Manuel Bareiro. We are grateful for the financial and practical support from the Centro Austral de Investigaciones Científicas del Consejo Nacional de Investigaciones Científicas y Técnicas (CADIC-CONICET), Argentina, and the Department of Archaeology and Cultural History (IAK) at the Norwegian University of Science and Technology (NTNU) University Museum, Norway. Thanks also to the four anonymous reviewers for their useful comments on our paper.

Disclosure statement

No potential conflict of interest was reported by the author(s).

Funding

This work was supported by the Research Council of Norway (RCN) under Grant 208828 (Marine Ventures); Agencia Nacional de Promoción de la Investigación, el Desarollo Tecnológico y la Innovacion (Agencia I + D + i), Proyectos de Investigación Científica y Tecnológica (PICT), under Grants PICT 2017 1230 and PICT-2021-I-A-00932; Centro Austral de Investigaciones Científicas, Consejo Nacional de Investigaciones Científicas y Técnicas (CADIC-CONICET), Argentina; and the Department of Archaeology and Cultural History, NTNU University Museum, Norwegian University of Science and Technology (NTNU).

ORCID

Jo Sindre P. Eidshaug http://orcid.org/0000-0001-9693-5254
Hein B. Bjerck http://orcid.org/0000-0003-2851-5981
Heidi M. Breivik http://orcid.org/0000-0002-9849-5173
Ole Risbøl http://orcid.org/0000-0003-1891-1868
Angélica M. Tivoli http://orcid.org/0000-0003-2283-5052
Atilio Francisco J. Zangrando http://orcid.org/0000-0002-5212-0894

Data availability statement

The ground survey data that support the findings of this study are openly available in NTNU Open at http://hdl.handle.net/11250/2428636. UAV LiDAR data are available from the corresponding author, JSPE, upon reasonable request. Open access satellite data were derived from the following resources available in the public domain: Google Earth (https://earth.google.com), ESRI World Imagery Wayback (https://livingatlas.arcgis.com/wayback), and Microsoft Bing Maps (https://www.bing.com/maps).

References

Agapiou, A., D. D. Alexakis, A. Sarris, and D. G. Hadjimitsis. 2014. Evaluating the potentials of Sentinel-2 for archaeological perspective. *Remote Sensing* 6 (3):2176–94. doi:10.3390/rs6032176

Alunni, D. V., A. M. Tivoli, and A. F. J. Zangrando. 2020. Movilidad y explotación de recursos terrestres por cazadores-recolectores costeros de Bahía Moat, costa sureste de Tierra del Fuego, Argentina [Mobility and exploitation of terrestrial resources by coastal hunter-gatherers of

Moat Bay, southeastern coast of Tierra del Fuego, Argentina]. *Latin American Antiquity* 31 (3):576–94. doi:10.1017/laq.2020.27

Barbour, T. E., K. E. Sassaman, A. M. A. Zambrano, E. N. Broadbent, B. Wilkinson, and R. Kanaski. 2019. Rare pre-Columbian settlement on the Florida Gulf Coast revealed through high-resolution drone LiDAR. *Proceedings of the National Academy of Sciences of the United States of America* 116 (47):23493–8. doi:10.1073/pnas.1911285116

Barceló, J. A., E. L. Piana, and D. R. Martinioni. 2002. Archaeological spatial modelling: A case study from Beagle Channel (Argentina). In *Archaeological informatics: Pushing the envelope. CAA 2001, Computer Applications and Quantitative Methods in Archaeology. Proceedings of the 29th Conference, Gotland, April 2001*, ed. G. Burenhult and J. Arvidsson, 351–60. Oxford: Archaeopress.

Barclay, W. S. 1926. *The land of Magellan*. London: Methuen.

Beck, A., G. Philip, M. Abdulkarim, and D. Donoghue. 2007. Evaluation of Corona and Ikonos high resolution satellite imagery for archaeological prospection in western Syria. *Antiquity* 81 (311):161–75. doi:10.1017/S0003598X00094916

Benker, S. C., R. P. Langford, and T. L. Pavlis. 2011. Positional accuracy of the Google Earth terrain model derived from stratigraphic unconformities in the Big Bend region, Texas, USA. *Geocarto International* 26 (4):291–303. doi:10.1080/10106049.2011.568125

Bevan, A. 2015. The data deluge. *Antiquity* 89 (348):1473–84. doi:10.15184/aqy.2015.102

Bewley, R., A. Wilson, D. Kennedy, D. Mattingly, R. Banks, M. Bishop, J. Bradbury, E. Cunliffe, M. Fradley, R. Jennings, et al. 2016. Endangered archaeology in the Middle East and North Africa: Introducing the EAMENA Project. In *CAA 2015: Keep the revolution going. Proceedings of the 43rd Annual Conference on Computer Applications and Quantitative Methods in Archaeology*, ed. S. Campana, R. Scopigno, G. Carpentiero, and M. Cirillo, 919–32. Oxford: Archaeopress.

Bird, J. 1938. Antiquity and migrations of the early inhabitants of Patagonia. *Geographical Review* 28 (2):250–75. doi:10.2307/210474

Bjerck, H. B. 2009. Colonizing seascapes: Comparative perspectives on the development of maritime relations in Scandinavia and Patagonia. *Arctic Anthropology* 46 (1–2):118–31. doi:10.1353/arc.0.0019

Bjerck, H. B. 2017. Settlements and seafaring: Reflections on the integration of boats and settlements among marine foragers in early Mesolithic Norway and the Yámana of Tierra del Fuego. *The Journal of Island and Coastal Archaeology* 12 (2):276–99. doi:10.1080/15564894.2016.1190425

Bjerck, H. B. 2021. What could the "sea ice machine" do to its people? On Lateglacial Doggerland, marine foraging, and colonisation of Scandinavian seascapes. *Environmental Archaeology* 26 (1):51–63. doi:10.1080/14614103.2019.1642673

Bjerck, H. B., H. M. Breivik, S. E. Fretheim, E. L. Piana, B. Skar, A. M. Tivoli, and A. F. J. Zangrando, eds. 2016. *Marine ventures: Archaeological perspectives on human–sea relations*. Sheffield: Equinox.

Bjerck, H. B., and A. F. J. Zangrando. 2013. Marine Ventures: Comparative perspectives on the dynamics of early human approaches to the seascapes of Tierra del Fuego and Norway. *The Journal of Island and Coastal Archaeology* 8 (1):79–90. doi:10.1080/15564894.2012.756083

Bjerck, H. B., and A. F. J. Zangrando. 2016. Introduction: Marine ventures—archaeological perspectives on human–sea relations. In *Marine ventures: Archaeological perspectives on human–sea relations*, ed. H. B. Bjerck, H. M. Breivik, S. E. Fretheim, E. L. Piana, B. Skar, A. M. Tivoli, and A. F. J. Zangrando, 5–14. Sheffield: Equinox.

Bjerck, H. B., A. F. J. Zangrando, H. M. Breivik, E. L. Piana, and J. Negre. 2016. Marine Ventures: The Cambaceres surveys, Tierra del Fuego, Argentina. NTNU University Museum report 2016:15. NTNU University Museum, Trondheim. Accessed July 2, 2018. http://hdl.handle.net/11250/2428636.

Björck, S., K. Lambeck, P. Möller, N. Waldmann, O. Bennike, H. Jiang, D. Li, P. Sandgren, A. B. Nielsen, and C. T. Porter. 2021. Relative sea level changes and glacio-isostatic modelling in the

Beagle Channel, Tierra del Fuego, Chile: Glacial and tectonic implications. *Quaternary Science Reviews* 251:106657. doi:10.1016/j.quascirev.2020.106657

Borie, C., C. Parcero-Oubiña, Y. Kwon, D. Salazar, C. Flores, L. Olguín, and P. Andrade. 2019. Beyond site detection: The role of satellite remote sensing in analysing archaeological problems. A case study in lithic resource procurement in the Atacama Desert, northern Chile. *Remote Sensing* 11 (7):869. doi:10.3390/rs11070869

Borrero, L. A., and F. M. Martin. 2023. Fragmented records: Fuego-Patagonian hunter-gatherers and archaeological change. In *Archaeology on the threshold: Studies in the processes of change*, ed. J. D. Wardle, R. K. Hitchcock, M. Schmader, and P.-L. Yu, 68–88. Gainesville: University Press of Florida.

Borrero, L. A., F. Morello, and M. San Román. 2020. Geografía cultural de los archipiélagos de Fuego-Patagonia en tiempos recientes: Movilidad y planificación [Cultural geography of the Fuegian-Patagonian archipelagos in recent times: Mobility and planning]. *Magellania* 48 (2): 45–70. doi:10.4067/S0718-22442020000200045

Bridges, E. L. 2007. *Uttermost part of the Earth: A history of Tierra del Fuego and the Fuegians*. New York: The Rookery Press.

Bridges, T. 1866. Manners and customs of the Firelanders. *A Voice for South America* 13:201–14.

Bridges, T. 1893. La Tierra del Fuego y sus habitantes [Tierra del Fuego and its habitants]. *Boletin del Instituto Geográfico Argentino* 14:221–41.

Bridges, T. 1987. *Yamana–English: A dictionary of the speech of Tierra del Fuego*. Buenos Aires: Zagier y Urrutu.

Buma, B., F. Morello, K. Rodriguez, and A. S. Fillol. 2022. Evidence for the southernmost pre-industrial human expansion on Isla Hornos (Isla Lököshpi), Chile. *Antiquity* 96 (389):1324–9. doi:10.15184/aqy.2022.91

Casana, J. 2021. Rethinking the landscape: Emerging approaches to archaeological remote sensing. *Annual Review of Anthropology* 50 (1):167–86. doi:10.1146/annurev-anthro-101819-110344

Casana, J., E. J. Laugier, A. C. Hill, K. M. Reese, C. Ferwerda, M. D. McCoy, and T. Ladefoged. 2021. Exploring archaeological landscapes using drone-acquired lidar: Case studies from Hawai'i, Colorado, and New Hampshire, USA. *Journal of Archaeological Science: Reports* 39: 103133. doi:10.1016/j.jasrep.2021.103133

Chapman, A., and T. R. Hester. 1973. New data on the archaeology of the Haush, Tierra del Fuego. *Journal de la Société des Américanistes* 62 (1):185–208. doi:10.3406/jsa.1973.2088

Chase, A., D. Z. Chase, C. T. Fisher, S. J. Leisz, and J. F. Weishampel. 2012. Geospatial revolution and remote sensing LiDAR in Mesoamerican archaeology. *Proceedings of the National Academy of Sciences of the United States of America* 109 (32):12916–21. doi:10.1073/pnas.1205198109

Cohen, A. S., S. Klassen, and D. H. Evans. 2020. Ethics in archaeological LiDAR. *Journal of Computer Applications in Archaeology* 3 (1):76–91. doi:10.5334/jcaa.48

Colonese, A. C., E. Verdún-Castelló, M. Álvarez, I. Briz I Godino, D. Zurro, and L. Salvatelli. 2012. Oxygen isotopic composition of limpet shells from the Beagle Channel: Implications for seasonal studies in shell middens of Tierra del Fuego. *Journal of Archaeological Science* 39 (6): 1738–48. doi:10.1016/j.jas.2012.01.012

Comer, D. C., and M. J. Harrower. 2012. *Mapping archaeological landscapes from space*. New York: Springer.

Contreas, D. A. 2010. Huaqueros and remote sensing imagery: Assessing looting damage in the Virú Valley, Peru. *Antiquity* 84 (324):544–55.

Corbat, M., A. M. Tivoli, and A. F. J. Zangrando. 2020. Aprovisionamiento de peces en el extremo oriental del canal Beagle (Tierra del Fuego, Argentina): Una evaluación a partir del registro zooarqueológico de Bahía Moat [Fish provisioning in the eastern end of the Beagle Channel (Tierra del Fuego, Argentina): An evaluation based on the zooarchaeological record of Moat Bay]. *Archaeofauna* 29:41–57. doi:10.15366/archaeofauna2020.29.003

Davis, D. S., G. Caspari, C. P. Lipo, and M. C. Sanger. 2021. Deep learning reveals extent of Archaic Native American shell-ring building practices. *Journal of Archaeological Science* 132: 105433. doi:10.1016/j.jas.2021.105433

Davis, D. S., and K. Douglass. 2020. Aerial and spaceborne remote sensing in African archaeology: A review of current research and potential future avenues. *African Archaeological Review* 37 (1):9–24. doi:10.1007/s10437-020-09373-y

Davis, D. S., C. P. Lipo, and M. C. Sanger. 2019. A comparison of automated object extraction methods for mound and shell-ring identification in coastal South Carolina. *Journal of Archaeological Science: Reports* 23:166–77. doi:10.1016/j.jasrep.2018.10.035

Davis, D. S., M. C. Sanger, and C. P. Lipo. 2019. Automated mound detection using LiDAR and object-based image analysis in Beaufort County, South Carolina. *Southeastern Archaeology* 38 (1):23–37. doi:10.1080/0734578X.2018.1482186

Doneus, M. 2013. Openness as visualization technique for interpretative mapping of airborne LiDAR derived digital terrain models. *Remote Sensing* 5 (12):6427–42. doi:10.3390/rs5126427

Doneus, M., Ł. Banaszek, and G. J. Verhoeven. 2022. The impact of vegetation on the visibility of archaeological features in airborne laser scanning datasets from different acquisition dates. *Remote Sensing* 14 (4):858. doi:10.3390/rs14040858

Doneus, M., and C. Briese. 2011. Airborne laser scanning in forested areas: Potential and limitations of an archaeological prospection technique. In *Remote sensing for archaeological heritage management. Proceedings of the 11th EAC Heritage Management Symposium, Reykjavík, Iceland, 25–27 March 2010*, ed. D. C. Cowley, 59–76. Brussels: Europae Archaeologia Consilium (EAC), Association Internationale sans But Lucratif (AISBL), Siège social.

Eidshaug, J. S. P., H. B. Bjerck, T. Lohndal, and O. Risbøl. 2024. Words as archaeological objects: A study of marine lifeways, seascapes, and coastal environmental knowledge in the Yagan–English dictionary. *International Journal of Historical Archaeology* 28 (3):722–66. doi:10.1007/s10761-024-00729-7

Emmitt, J., K. Allely, B. Davies, E. Hoffman, and S. J. Holdaway. 2020. Preliminary archaeological survey and remote-sensing of shell mounds at Kwokkunum, Albatross Bay, Cape York Peninsula, Australia. *Queensland Archaeological Research* 23:9–24. doi:10.25120/qar.23.2020.3718

Erlandson, J. M. 2008. Racing a rising tide: Global warming, rising seas, and the erosion of human history. *The Journal of Island and Coastal Archaeology* 3 (2):167–9. doi:10.1080/15564890802436766

Erlandson, J. M. 2012. As the world warms: Rising seas, coastal archaeology, and the erosion of maritime history. *Journal of Coastal Conservation* 16 (2):137–42. doi:10.1007/s11852-010-0104-5

Erlandson, J. M., K. M. Gill, A. E. Gusick, and A. E. Dorrler. 2019. Identifying shell middens with historic aerial photos: An example from California's Santa Cruz Island. *The Journal of Island and Coastal Archaeology* 14 (1):113–22. doi:10.1080/15564894.2017.1324926

Estevez, J., E. Piana, A. Schiavini, and N. Juan-Muns. 2001. Archaeological analysis of shell middens in the Beagle Channel, Tierra del Fuego Island. *International Journal of Osteoarchaeology* 11 (1–2):24–33. doi:10.1002/oa.543

Evans, D. H., R. J. Fletcher, C. Pottier, J.-B. Chevance, D. Soutif, B. S. Tan, S. Im, D. Ea, T. Tin, S. Kim, et al. 2013. Uncovering archaeological landscapes at Angkor using LiDAR. *Proceedings of the National Academy of Sciences of the United States of America* 110 (31):12595–600. doi:10.1073/pnas.1306539110

Fretheim, S. E., E. L. Piana, H. B. Bjerck, and A. F. J. Zangrando. 2016. Home by the sea: Exploring traditions of dwelling reoccupation and settlement stability among marine foragers in Norway and Tierra del Fuego. In *Marine ventures: Archaeological perspectives on human–sea relations*, ed. H. B. Bjerck, H. M. Breivik, S. E. Fretheim, E. L. Piana, B. Skar, A. M. Tivoli, and A. F. J. Zangrando, 175–92. Sheffield: Equinox.

Gallardo, F., G. Cabello, M. Sepúlveda, B. Ballester, D. Fiore, and A. Prieto. 2023. Yendegaia Rockshelter, the first rock art site on Tierra del Fuego Island and social interaction in Southern Patagonia (South America). *Latin American Antiquity* 34 (3):532–49. doi:10.1017/laq.2022.47

Gattiglia, G. 2015. Thinking big about data: Archaeology and the big data challenge. *Archäologische Informationen* 38:113–24.

Gorelick, N., M. Hancher, M. Dixon, S. Ilyushchenko, D. Thau, and R. Moore. 2017. Google Earth Engine: Planetary-scale geospatial analysis for everyone. *Remote Sensing of Environment* 202:18–27. doi:10.1016/j.rse.2017.06.031

Gusinde, M. 1937. *Die Yamana* [The Yamana]. Vol. II. A of *Die Feuerland-Indianer* [The Fireland Indians]. Mödling bei Wien: Verlag der Internationalen Zeitschrift "Anthropos.".

Herndon, K. E., R. Griffin, W. Schroder, T. Murtha, C. Golden, D. A. Contreras, E. Cherrington, L. Wang, A. Bazarsky, G. V. Kollias, et al. 2023. Google Earth Engine for archaeologists: An updated look at the progress and promise of remotely sensed big data. *Journal of Archaeological Science: Reports* 50:104094. doi:10.1016/j.jasrep.2023.104094

Hesse, R. 2010. LiDAR-derived local relief models: A new tool for archaeological prospection. *Archaeological Prospection* 17 (2):67–72. doi:10.1002/arp.374

Hesse, R. 2016. Visualisierung hochauflösender Digitaler Geländemodelle mit LiVT [Visualization of high-resolution digital terrain models with LiVT]. In *Computeranwendungen und Quantitative Methoden in der Archäologie* [Computer applications and quantitative methods in archaeology], ed. U. Lieberwirth and I. Herzog, 109–28. Berlin: Topoi.

Horwitz, V. D., and M. N. Weissel. 2011. Arqueología de Isla de los Estados: La frontera de la abundancia [Archaeology of Isla de los Estados: The frontier of abundance]. In *Los cazadores-recolectores del extremo oriental fueguino: Arqueología de Península Mitre e Isla de los Estados* [The hunter-gatherers of the far eastern Tierra del Fuego: Archaeology of Peninsula Mitre and Isla de los Estados], ed. A. F. J. Zangrando, M. Vázquez, and A. Tessone, 143–70. Buenos Aires: Sociedad Argentina de Antropología.

Howey, M. C. L., F. B. Sullivan, M. B. Burg, and M. W. Palace. 2020. Remotely sensed Big Data and iterative approaches to cultural feature detection and past landscape process analysis. *Journal of Field Archaeology* 45 (sup1):S27–S38. doi:10.1080/00934690.2020.1713435

Hritz, C. 2014. Contributions of GIS and satellite-based remote sensing to landscape archaeology in the Middle East. *Journal of Archaeological Research* 22 (3):229–76. doi:10.1007/s10814-013-9072-2

Huggett, J. 2020. Is big data different? Towards a new archaeological paradigm. *Journal of Field Archaeology* 45 (sup1):S8–S17. doi:10.1080/00934690.2020.1713281

Hyades, P. D., and J. Deniker. 1891. *Antropologie, ethnographie* [Anthropology, ethnography]. *Vol. VII of Mission scientifique du Cap Horn, 1882–1883* [Scientific mission to Cape Horn, 1882–1883]. Paris: Gauthier-Villars et Fils.

Ingold, T. 2007. Earth, sky, wind, and weather. *Journal of the Royal Anthropological Institute* 13 (s1):S19–S38. doi:10.1111/j.1467-9655.2007.00401.x

Iriarte, J., M. Robinson, J. de Souza, A. Damasceno, F. da Silva, F. Nakahara, A. Ranzi, and L. Aragao. 2020. Geometry by design: Contribution of LiDAR to the understanding of settlement patterns of the mound villages in SW Amazonia. *Journal of Computer Applications in Archaeology* 3 (1):151–69. doi:10.5334/jcaa.45

Kempe, S., and A. Al-Malabeh. 2013. Desert kites in Jordan and Saudi Arabia: Structure, statistics and function, a Google Earth study. *Quaternary International* 297:126–46. doi:10.1016/j.quaint.2013.02.013

Kennedy, D., and M. C. Bishop. 2011. Google Earth and the archaeology of Saudi Arabia: A case study from the Jeddah area. *Journal of Archaeological Science* 38 (6):1284–93. doi:10.1016/j.jas.2011.01.003

Khalaf, N., and T. Insoll. 2019. Monitoring Islamic archaeological landscapes in Ethiopia using open source satellite imagery. *Journal of Field Archaeology* 44 (6):401–19. doi:10.1080/00934690.2019.1629256

Kokalj, Ž., and M. Somrak. 2019. Why not a single image? Combining visualizations to facilitate fieldwork and on-screen mapping. *Remote Sensing* 11 (7):747. doi:10.3390/rs11070747

Koppers, P. W. 1927. Die fünf Dialekte in der Sprache der Yamana auf Feuerland [The five dialects in language of the Yamana of Fireland]. *Anthropos* 22 (3/4):466–76.

Legoupil, D. 1993–1994. El archipiélago del Cabo de Hornos y la costa sur de la Isla Navarino: Poblamiento y modelos económicos [The Cape Horn archipelago and the southern coast of

Navarino Island: Settlement and economic models]. *Anales del Instituto de la Patagonia* 22: 101–21.

Legoupil, D. 2000. El sistema socioeconómico del los nómades del mar de Skyring (archipiélago de Patagonia) [The socio-economic system of the nomades of the sea of Skyring (Patagonian archipelago)]. *Anales del Instituto de la Patagonia* 28:81–119.

Lindsay, I., and A. Mkrtchyan. 2023. Free and low-cost aerial remote sensing in archaeology: An overview of data sources and recent applications in the South Caucasus. *Advances in Archaeological Practice* 11 (2):164–83. doi:10.1017/aap.2023.3

Lothrop, S. K. 1928. *The Indians of Tierra del Fuego: An account of the Ona, Yaghan, Alacaluf and Haush natives of the Fuegian archipelago*. New York: Museum of the American Indian Heye Foundation.

Luo, L., X. Wang, H. Guo, R. Lasaponara, P. Shi, N. Bachagha, L. Li, Y. Yao, N. Masini, F. Chen, et al. 2018. Google Earth as a powerful tool for archaeological and cultural heritage applications: A review. *Remote Sensing* 10 (10):1558. doi:10.3390/rs10101558

Luo, L., X. Wang, H. Guo, R. Lasaponara, X. Zong, N. Masini, G. Wang, P. Shi, H. Khatteli, F. Chen, et al. 2019. Airborne and spaceborne remote sensing for archaeological and cultural heritage applications: A review of the century (1907–2017). *Remote Sensing of Environment* 232:111280. doi:10.1016/j.rse.2019.111280

Luo, L., X. Wang, J. Liu, W. Zheng, J. Zhen, L. Zhu, C. Liu, and H. Wan. 2019. Low-cost archaeological investigation and rapid mapping of ancient stone tidal weirs in the Penghu Archipelago using Google Earth. *Sustainability* 11 (17):4536. doi:10.3390/su11174536

Lyman, R. L. 1991. *Prehistory of the Oregon coast: The effects of excavation strategies and assemblage size on archaeological inquiry*. New York: Academic Press.

Martial, L. F. 1888. *Histoire du voyages* [History of traveling]. *Vol. I of Mission scientifique du Cap Horn, 1882–1883* [Scientific mission to Cape Horn, 1882–3]. Paris: Gauthier-Villars.

Martinic, M. 1989. Los canoeros de la Patagonia Meridional: Población histórica y distribución geográfica (siglos XIX y XX). El fin de una etnia [The canoe people of southern Patagonia: Settlement history and geographic distribution (19th and 20th centuries). The end of an ethnic group]. *Journal de la Société des Américanistes* 75: 35–61.

Masini, N., F. T. Gizzi, M. Biscione, V. Fundone, M. Sedile, M. Sileo, A. Pecci, B. Lacovara, and R. Lasaponara. 2018. Medieval archaeology under the canopy with LiDAR: The (re)discovery of a Medieval fortified settlement in Southern Italy. *Remote Sensing* 10 (10):1598. doi:10.3390/rs10101598

Mayer-Schönberger, V., and K. Cukier. 2013. *Big data: A revolution that will transform how we live, work, and think*. Boston: Houghton Mifflin Harcourt.

Menze, B. H., and J. A. Ur. 2012. Mapping patterns of long-term settlement in Northern Mesopotamia at a large scale. *Proceedings of the National Academy of Sciences of the United States of America*. 109 (14):E778–87.

O'Reilly, D. J. W., and G. Scott. 2015. Moated sites of the Iron Age in the Mun River Valley, Thailand: New discoveries using Google Earth. *Archaeological Research in Asia* 3:9–18. doi:10.1016/j.ara.2015.06.001

Ocampo, C., and P. Rivas. 2002. Arqueología del Canal Beagle: Secuencias y procesos culturales en ambientes de altas latitudes [Archaeology of the Beagle Channel: Sequences and cultural processes in high-latitude environments]. *Boletín de la Sociedad Chilena de Arqeuología* 33/34: 98–102.

Ocampo, C., and P. Rivas. 2004. Poblamiento temprano de los extremos geográficos de los canales Patagónicos: Chiloé e Isla Navarino 1 [Early settlement of the geographical extremes of the Patagonian channels: Chiloé and Navarino Island 1]. *Chungará Revista de Antropología Chilena* 36 (sup):317–31.

Oltean, I. A., and L. L. Abell. 2012. High-resolution satellite imagery and the detection of buried archaeological features in ploughed landscapes. In *Satellite remote sensing: A new tool for archaeology*, ed. R. Lasaponara and N. Masini, 291–305. Dordrecht: Springer.

Opitz, R. S., and D. C. Cowley. 2013. *Interpreting archaeological topography: 3D data, visualisation and observation*. Oxford: Oxbow.

Orquera, L. A., D. Legoupil, and E. L. Piana. 2011. Littoral adaptation at the southern end of South America. *Quaternary International* 239 (1–2):61–9. doi:10.1016/j.quaint.2011.02.032

Orquera, L. A., and E. L. Piana. 1996. El sitio Shamakush I (Tierra del Fuego, República Argentina) [The Shamakush I site (Tierra del Fuego, Republic of Argentina)]. *Relaciones de la Sociedad Argentina de Antropología* 21:215–65.

Orquera, L. A., and E. L. Piana. 1999. *Arqueología de la región del canal Beagle (Tierra del Fuego, República Argentina)* [Archaeology of the Beagle Channel region (Tierra del Fuego, Republic of Argentina)]. Buenos Aires: Sociedad Argentina de Antropología.

Orquera, L. A., and E. L. Piana. 2009. Sea nomads of the Beagle Channel in southernmost South America: Over six thousand years of coastal adaptation and stability. *The Journal of Island and Coastal Archaeology* 4 (1):61–81. doi:10.1080/15564890902789882

Orquera, L. A., and E. L. Piana. 2015. *La vida material y social de los Yámana* [The material and social life of the Yamana]. Corrected and augmented ed. Ushuaia: Monte Olivia.

Orquera, L. A., and E. L. Piana. 2020. Calibración radiocarbónica en la región del Canal Beagle [Radiocarbon calibration in the Bealge Channel region]. *Relaciones de la Sociedad Argentina de Antropología* 15 (1):201–21.

Parcak, S., D. Gathings, C. Childs, G. Mumford, and E. Cline. 2016. Satellite evidence of archaeological site looting in Egypt: 2002–2013. *Antiquity* 90 (349):188–205. doi:10.15184/aqy.2016.1

Paredes-Hernández, C. U., W. E. Salinas-Castillo, F. Guevara-Cortina, and X. Martínez-Becerra. 2013. Horizontal positional accuracy of Google Earth's imagery over rural areas: A study case in Tamaulipas, Mexico. *Boletim de Ciências Geodésicas* 19 (4):588–601. doi:10.1590/S1982-21702013000400005

Pérez, S. A., A. Tessone, and A. F. J. Zangrando. 2022. Metodología multi-proxy aplicada al estudio de la formación de concheros en el canal Beagle [Multi-proxy methodology applied in the study of shell midden formations in the Beagle Channel]. Paper presented at the 6° Congreso Nacional de Zooarqueología Argentina, La Plata, November 14.

Piana, E. L., and L. A. Orquera. 2010. Shellmidden formation at the Beagle Channel (Tierra del Fuego, Argentine. In *Monumental questions: Prehistoric megaliths, mounds, and enclosures. Proceedings of the XV World Congress (Lisbon, 4–9 September 2006)*, ed. D. Calado, M. Baldia, and M. Boulanger, 263–72. Oxford: Archaeopress.

Pulighe, G., V. Baiocchi, and F. Lupia. 2016. Horizontal accuracy assessment of very high resolution Google Earth images in the city of Rome, Italy. *International Journal of Digital Earth* 9 (4):342–62. doi:10.1080/17538947.2015.1031716

Randall, A. R. 2014. LiDAR-aided reconnaissance and reconstruction of lost landscapes: An example of freshwater shell mounds (ca. 7500–500 cal b.p.) in northeastern Florida. *Journal of Field Archaeology* 39 (2):162–79. doi:10.1179/0093469014Z.00000000080

Ranzi, A., R. Feres, and F. Brown. 2007. Internet software programs aid in search for Amazonian geoglyphs. *Eos, Transactions American Geophysical Union* 88 (21):226–9. doi:10.1029/2007EO210003

Rick, T. C. 2024. Shell midden archaeology: Current trends and future directions. *Journal of Archaeological Research* 32 (3):309–66. doi:10.1007/s10814-023-09189-9.

Risbøl, O. 2013. Cultivating the "wilderness": How LiDAR can improve archaeological landscape understanding. In *Interpreting archaeological topography: 3D data, visualisation and observation*, ed. R. S. Opitz and D. C. Cowley, 51–62. Oxford: Oxbow.

Risbøl, O., J. S. P. Eidshaug, H. B. Bjerck, M. M. Gran, K. R. Rantala, A. M. Tivoli, and A. F. J. Zangrando. 2023. UAV LiDAR in coastal environments: Archaeological case studies from Tierra del Fuego, Argentina, and Vega, Norway. *Archaeological Prospection* 30 (4):533–57. doi:10.1002/arp.1918

Sadr, K. 2016. A comparison of accuracy and precision in remote sensing stone-walled structures with Google Earth, high resolution aerial photography and LiDAR: A case study from the South African Iron Age. *Archaeological Prospection* 23 (2):95–104. doi:10.1002/arp.1532

San Román, M., O. Reyes, J. Torres, and F. Morello. 2016. Archaeology of maritime hunter-gatherers from southernmost Patagonia, South America: Discussing timing, changes and cultural traditions during the Holocene. In *Marine ventures: Archaeological perspectives on human–sea*

relations, ed. H. B. Bjerck, H. M. Breivik, S. E. Fretheim, E. L. Piana, B. Skar, A. M. Tivoli, and A. F. J. Zangrando, 157–74. Sheffield: Equinox.

Snyder, T. J., and R. Haas. 2024. Unstructured satellite survey detects up to 20% of archaeological sites in coastal valleys of southern Peru. *PLoS One* 19 (2):e0292272. doi:10.1371/journal.pone.0292272

Stoner, W. D. 2017. Risk, agricultural intensification, political administration, and collapse in the classic period gulf lowlands: A view from above. *Journal of Archaeological Science* 80:83–95. doi:10.1016/j.jas.2017.02.002

Stott, D., S. M. Kristiansen, and S. M. Sindbæk. 2019. Searching for Viking Age fortresses with automatic landscape classification and feature detection. *Remote Sensing* 11 (16):1881. doi:10.3390/rs11161881

Thuestad, A. E., O. Risbøl, J. I. Kleppe, S. Barlindhaug, and E. R. Myrvoll. 2021. Archaeological surveying of subarctic and arctic landscapes: Comparing the performance of airborne laser scanning and remote sensing image data. *Sustainability* 13 (4):1917. doi:10.3390/su13041917

Tivoli, A., M. A. Montes, D. V. Alunni, M. d. C. Fernández Ropero, M. P. Martinoli, S. A. Pérez, G. Pinto Vargas, R. López, R. Saenz Samaniego, et al. 2022. Arqueología de sectores insulares en el canal Beagle (Argentina): El caso del archipiélago de las islas Bridges e islas adyacentes [Archaeology of insular sectors in the Beagle Channel (Argentina): The case of the archipelago of Bridges Islands and adjacent islands]. *Arqueología* 28 (1):9976. doi:10.34096/arqueologia.t28.n1.9976

Tivoli, A. M., and A. F. J. Zangrando. 2011. Subsistence variations and landscape use among maritime hunter-gatherers: A zooarchaeological analysis from the Beagle Channel (Tierra del Fuego, Argentina). *Journal of Archaeological Science* 38 (5):1148–56. doi:10.1016/j.jas.2010.12.018

Vázquez, M., A. F. J. Zangrando, A. Tessone, and A. Ceraso. 2011. Arqueología de la costa meridional de Península Mitre [Archaeology of the southern coast of Peninsula Mitre]. In *Los cazadores-recolectores del extremo oriental fueguino: Arqueología de Península Mitre e Isla de los Estados* [The hunter-gatherers of the far eastern Tierra del Fuego: Archaeology of Peninsula Mitre and Isla de los Estados], ed. A. F. J. Zangrando, M. Vázquez, and A. Tessone, 203–30. Buenos Aires: Sociedad Argentina de Antropología.

Vázquez, M., A. F. J. Zangrando, A. Tessone, A. Ceraso, and L. Sosa. 2007. Arqueología de Bahía Valentin (Península Mitre, Tierra del Fuego): Nuevos resultados y perspectivas [Archaeology of Valentin Bay (Peninsula Mitre, Tierra del Fuego): New results and perspectives]. In *Arqueología de Fuego-Patagonia: Levantando piedras, desenterrando huesos… y develando arcanos* [Archaeology of Fuego-Patagonia: Lifting stones, unearthing bones…and unveiling secrets], ed. F. Morello, M. Martinic, A. Prieto, and G. Bahamonde, 755–66. Punta Arenas: Centro de Estudios del Cuaternario Antártico (CEQUA).

Vidal, H. J. 2011. El conocimiento de las culturas aborígenes del sudeste de la Isla Grande hasta 1983 [Knowledge of the aboriginal cultures of the southeast of Isla Grande until 1983]. In *Los cazadores-recolectores del extremo oriental fueguino: Arqueología de Península Mitre e Isla de los Estados* [The hunter-gatherers of the far eastern Tierra del Fuego: Archaeology of Peninsula Mitre and Isla de los Estados], ed. A. F. J. Zangrando, M. Vázquez, and A. Tessone, 65–114. Buenos Aires: Sociedad Argentina de Antropología.

Vinci, G., F. Vanzani, A. Fontana, and S. Campana. 2024. LiDAR applications in archaeology: A systematic review. *Archaeological Prospection*. doi:10.1002/arp.1931.

Waselkov, G. A. 1987. Shellfish gathering and shell midden archaeology. *Advances in Archaeological Method and Theory* 10:93–210.

Zakšek, K., K. Oštir, and Ž. Kokalj. 2011. Sky-view factor as a relief visualization technique. *Remote Sensing* 3 (2):398–415. doi:10.3390/rs3020398

Zangrando, A. F. J. 2010. Coastal archaeology and hunter-gatherers in southeastern Tierra del Fuego. *The Journal of Island and Coastal Archaeology* 5 (2):288–91. doi:10.1080/15564894.2010.487360

Zangrando, A. F. J. 2018. Shell middens and coastal archaeology in southern South America. In *Encyclopedia of global archaeology*, ed. C. Smith, 1–15. Cham: Springer.

Zangrando, A. F. J., K. B. Borrazzo, A. M. Tivoli, D. V. Alunni, and M. P. Martinoli. 2014. El sitio Heshkaia 35: Nuevos datos sobre la arqueología de Moat (Tierra del Fuego, Argentina) [The Heshkaia 35 site: New data about the archaeology of Moat (Tierra del Fuego, Argentina)]. *Revista del Museo de Antropología* 7 (1):11–24. doi:10.31048/1852.4826.v7.n1.9090

Zangrando, A. F. J., J. F. Ponce, M. P. Martinoli, A. Montes, E. L. Piana, and F. Vanella. 2016. Palaeogeographic changes drove prehistoric fishing practices in the Cambaceres Bay (Tierra del Fuego, Argentina) during the middle and late Holocene. *Environmental Archaeology* 21 (2): 182–92. doi:10.1080/14614103.2015.1130888

Zangrando, A. F. J., A. M. Tivoli, J. F. Ponce, D. V. Alunni, M. del, C. Fernández Ropero, and M. P. Martinoli. 2022. Colonización humana de Tierra del Fuego: Contextos arqueológicos pretransgresivos en la costa norte del Canal Beagle [Human colonization of Tierra del Fuego: Pre-transgresive archaeological contexts of the northern coast of the Beagle Channel]. *Chungara Revista de Antropología Chilena* 54 (3):557–77.

Zangrando, A. F. J., M. Vázquez, and A. Tessone. 2011. Arqueología de Península Mitre e Isla de los Estados: Una introducción [Archaeology of Peninsula Mitre and Isla de los Estados: An introduction]. In *Los cazadores-recolectores del extremo oriental fueguino: Arqueología de Península Mitre e Isla de los Estados* [The hunter-gatherers of the far eastern Tierra del Fuego: Archaeology of Peninsula Mitre and Isla de los Estados], ed. A. F. J. Zangrando, M. Vázquez, and A. Tessone, 19–30. Buenos Aires: Sociedad Argentina de Antropología.